Lie symmetry analysis of flow and heat transfer in an inclined deformable channel under the influence of magnetic field during filtration process

ML Lekoko

orcid.org 0000-0002-6732-6048

Dissertation accepted in partial fulfilment of the requirements for the degree *Master of Science in Applied Mathematics* at the North-West University

Supervisor: Dr G Magalakwe

Graduation May 2020

23192267

LIE SYMMETRY ANALYSIS OF FLOW AND HEAT TRANSFER IN AN INCLINED DEFORMABLE CHANNEL UNDER THE INFLUENCE OF MAGNETIC FIELD DURING FILTRATION PROCESS

by

Lucas Lekoko (23192267)

A research project submitted in partial fulfilment
of the requirements for a masters degree in
Applied Mathematics at
North-West University, Potchefstroom Campus.

Department of Mathematics and Applied Mathematics
Faculty of Natural and Agricultural Sciences
North-West University
November, 2019

Supervision by Dr. Gabriel Magalakwe

The financial assistance of CSIR-DST-interbursary
programme towards this research is hereby acknowledged.
Opinions expressed and conclusions arrived at, are those of the author and are not
necessarily to be attributed to the CSIR.

Declaration

I hereby declare that the work in this mini-dissertation is my own work beside where references used have been acknowledged. No part of this mini-dissertation has been submitted for any qualification previously at North-West University or any other institution.

Signed by: ....

MR MODISAWATSONA LUCAS LEKOKO

Date: ....

This mini-dissertation has been submitted with my approval as a University supervisor and would certify that the requirements for the applicable Masters degree rules and regulations have been fulfilled.

Signed by:..

DR GABRIEL MAGALAKWE

Date: ....

Dedication

My humble efforts are dedicated to my girlfriend and supportive family whose remarkable support, prayers and words of encouragement which led to the accomplishment of this mini-dissertation.

Acknowledgement

I thank Dr Gabriel Magalakwe for his invaluable assistance and insights which led to completion and writing of this project. My sincere thanks also goes to the members of postgraduate committee for their patience, understanding and support during the two year period of efforts that went into this project.

My gratitude goes to the CSIR-DST inter-bursary programme for providing me with funding during the duration of my study. Lastly, above all, I would like to praise and thank God, the almighty, for his presence and grace throughout my mini-dissertation until its completion.

Abstract

This project seeks to investigate the effects of dimensionless parameters affecting flow dynamics and heat distribution during filtration process which leads to optimal out flow (maximum permeates). The study carried out a detailed mathematical modeling process based on conservation of mass, momentum and energy to construct mathematical representation of flow and heat transfer during filtration process. Also dimensionless parameters that affect the flow dynamics and heat distribution are indicated based on the design of the filter. To understand the dynamics of underlying study better, basic governing partial differential equations representing the internal flow and heat transfer are reduced to a system of ordinary differential equations by using the Lie symmetry analysis. Thereafter, double perturbation is used to approximate solutions of velocity variation and heat distribution inside the filter chamber analytically. Results are presented graphically for effects of parameter affecting the flow dynamics and heat distribution. Also analysis is carried out to obtain combination of parameters that lead to optimal filtration process.

Key words: MHD flow; magnetic field; thermal radiation; buoyancy effects; stable filtration process; Lie group analysis; perturbation method; conservation laws.

List of Symbols

NOMENCLATURE

c_p-specific heat, Jk/gK

$2h$-distance between walls, m

$\dot{h}$- wall dilation rate, m/s

$\bar{t}$-time, s

$\bar{u}$-axial-velocity, m/s

$\bar{v}$-normal-velocity, m/s

$\bar{x}$-axial coordinate, m

$\bar{y}$-normal coordinate, m

t-dimensionless time

u-dimensionless axial-velocity

v-dimensionless normal-velocity

x-dimensionless axial coordinate

y-dimensionless normal coordinate

$\bar{P}$-pressure, Pa

μ-dynamic viscosity, kg/ms

G_r-Grashoff number

g-gravitational acceleration, m/s^2

k-permeability of porous medium m^2

B_0-magnetic field strength Nm/A

P-dimensionless pressure

R_e-permeation Reynolds number

N-Stuart number

K-dimensionless porosity variable

T-temperature of the fluid, K

T_w- temperature at wall, K

T_h- temperature of the fluid at a certain height from the wall, K

ν-kinematic viscosity, m^2/s

P_r- Prandtl number

R-dimensionless radiation parameter

J-dimensionless Joule heating

Greek symbols

ρ-density, kg/m^3

Ψ-dimensionless stream function

ϕ-dimensionless porosity

$\bar{\Psi}$-stream function m^2/s

σ-electrical conductivity of fluid S/m

μ-magnetic permeability H/m

θ-dimensionless temperature function

α-thermal diffusion

γ-angle of inclination

subscrips

w-wall condition

h-fluid height

Contents

Introduction

Mathematical modelling by making use of basic conservation laws to formulate mathematical representation of flow behaviour and heat transfer in various fluid dynamics systems have received a considerable amount of attention in various fields of science and engineering. To understand momentum change and energy variation of various systems modelled by conservation laws, finding solutions of momentum and energy equations became critical part of research. Various techniques to obtain solutions of momentum and energy equations representing different scientific applications have also been established by researchers. Some of established techniques are homotopy analysis method [1], perturbation method [2], numerical methods [3] and Lie group methods [4] to mention a few.

Lie symmetry theory [4], by Sophus Lie gives an invariant transformations that preserve the dynamics of flow and heat transfer of systems modelled by conservations laws under a symmetry transformation. Lie's theory is known to be a powerful tool that conserves complicated dynamics when transforming a complex system to a simpler system. Lie symmetry technique has been applied to various areas of fluid dynamics since the method preserve the dynamics of the flow, see for example [2, 5, 6].

In this project, we consider a two-dimensional incompressible and electrically conducting viscous fluid in an inclined porous rectangular channel bounded by two permeable walls which represent internal flow and heat distribution during filtration process. To understand filtration process better, the current study further investigates the work of [7] by studying the effects of buoyancy force, magnetic field, radiation, Joule heating and angle of inclination on the internal flow and heat distribution. The equations representing the current case study are given by

$$\frac{\partial \bar{u}}{\partial \bar{x}}+\frac{\partial \bar{v}}{\partial \bar{y}}=0, \tag{1}$$

$$\frac{\partial \bar{u}}{\partial t}+\bar{u}\frac{\partial \bar{u}}{\partial \bar{x}}+\bar{v}\frac{\partial \bar{u}}{\partial \bar{y}}=-\frac{1}{\rho}\frac{\partial \bar{P}}{\partial \bar{x}}+\nu\left[\frac{\partial^2 \bar{u}}{\partial \bar{x}^2}+\frac{\partial^2 \bar{u}}{\partial \bar{y}^2}\right]-\frac{\nu\phi}{k}\bar{u}-\frac{\sigma B_0^2}{\rho}\bar{u}, \tag{2}$$

$$\begin{aligned}&\frac{\partial \bar{v}}{\partial t}+\bar{u}\frac{\partial \bar{v}}{\partial \bar{x}}+\bar{v}\frac{\partial \bar{v}}{\partial \bar{y}}=-\frac{1}{\rho}\frac{\partial \bar{P}}{\partial \bar{y}}+\nu\left[\frac{\partial^2 \bar{v}}{\partial \bar{x}^2}+\frac{\partial^2 \bar{v}}{\partial \bar{y}^2}\right]-\frac{\nu\phi}{k}\bar{v}\\&+g\beta(T-T_h)\cos(\gamma),\end{aligned} \tag{3}$$

$$\frac{\partial T}{\partial t}+\bar{u}\frac{\partial T}{\partial \bar{x}}+\bar{v}\frac{\partial T}{\partial \bar{y}}=\frac{\bar{k}}{\rho c_p}\left[\frac{\partial^2 T}{\partial \bar{x}^2}+\frac{\partial^2 T}{\partial \bar{y}^2}\right]-\frac{1}{\rho c_p}\frac{\partial q_r}{\partial \bar{y}}+\frac{\sigma B_0^2}{\rho c_p}\bar{u}^2 \tag{4}$$

together with the following boundary conditions

$$\begin{aligned}&\text{(i)} \quad \bar{u}=0, \quad \bar{v}=-V_w, \quad T=T_w \quad \text{at } \bar{y}=h(t),\\&\text{(ii)} \quad \frac{\partial \bar{u}}{\partial \bar{y}}=0, \quad \bar{v}=0, \quad \frac{\partial T}{\partial \bar{y}}=0 \quad \text{at } \bar{y}=0,\\&\text{(iii)} \quad \bar{u}=0 \quad \text{at } \bar{x}=0.\end{aligned} \tag{5}$$

This project uses Lie symmetry analysis and double perturbation to obtain approximate solutions that can be used to seek a combination of parameters affecting the process that yields optimal outflow (maximum permeates) during filtration process.

The layout of the mini-dissertation is as follows:

In Chapter one, we briefly provide an introduction to Lie symmetry analysis of partial differential equations and include the necessary results which will be used throughout this work. In particular, an algorithm to calculate symmetries of partial differential equations is given.

In Chapter two, we illustrate how to obtain symmetries of Burger's equation which has direct application in fluid dynamics. Also, we obtain the invariant solutions of the Burger's equation.

In Chapter three, we use Lie symmetry analysis together with perturbation method to study flow and heat transfer in an inclined deformable channel under the influence of magnetic field during filtration process.

Finally, in Chapter four we summarize the work done in this mini-dissertation. Bibliography is given at the end.

Chapter 1

Preliminaries

This chapter presents the algorithm to determine symmetries of partial differential equations, which will be used through out this mini-dissertation.

1.1 Introduction

Mathematical representations of real life phenomena evolve in both space and time, thus lead to partial differential equations. These equations representing real life phenomena can be difficult if not possible to solve analytically due to higher dimensions that differ from one phenomena to another. The Norwegian mathematician by the name of Sophus Lie, discovered a way to transform a system of such higher dimension to a simpler system while preserving the behaviour of the original system using Lie symmetry analysis more than hundred years ago. Lie symmetry analysis provides group of transforms that maps a partial differential equations to ordinary differential equations without changing the dynamics of the phenomenon represented by partial differential equations. Due to the importance of the method (Lie symmetry analysis) to differential equations several books have been written on this topic, see [4, 8–11] to mention a few. **The results and definitions below are from the books mentioned above and we will not refer to them again**.

1.2 Local one-parameter Lie group

Let $x = (x^1, ..., x^n)$ be the independent variables with coordinates x^i and $u = (u^1, ..., u^m)$ be the dependent variables with coordinates u^α (n and m finite). Consider a change of the variables x and u involving a real parameter a:

$$T_a : \bar{x^i} = f^i(x, u, a),\ \bar{u^\alpha} = \phi^\alpha(x, u, a), \tag{1.1}$$

where a continuously ranges in values from a neighborhood $\mathcal{D}' \subset \mathcal{D} \subset \mathbb{R}$ of $a = 0$, and f^i and ϕ^α are differentiable functions.

Definition 1.1 A set G of transformations (1.1) is called a *continuous one-parameter (local) Lie group of transformations* in the space of variables x and u if

(i) For $T_a,\ T_b \in G$ where $a, b \in \mathcal{D}' \subset \mathcal{D}$ then $T_b\,T_a = T_c \in G,\ c = \phi(a, b) \in \mathcal{D}$ (Closure)

(ii) $T_0 \in G$ if and only if $a = 0$ such that $T_0\,T_a = T_a\,T_0 = T_a$ (Identity)

(iii) For $T_a \in G,\ a \in \mathcal{D}' \subset \mathcal{D},\ T_a^{-1} = T_{a^{-1}} \in G,\ a^{-1} \in \mathcal{D}$ such that
$T_a\,T_{a^{-1}} = T_{a^{-1}}\,T_a = T_0$ (Inverse)

We note that the associativity property follows from (i). The group property (i) can be written as

$$\begin{aligned} \bar{\bar{x}}^i &\equiv f^i(\bar{x}, \bar{u}, b) = f^i(x, u, \phi(a, b)), \\ \bar{\bar{u}}^\alpha &\equiv \phi^\alpha(\bar{x}, \bar{u}, b) = \phi^\alpha(x, u, \phi(a, b)) \end{aligned} \tag{1.2}$$

and the function ϕ is called the *group composition law.* A group parameter a is called *canonical* if $\phi(a, b) = a + b$.

Theorem 1.1 For any $\phi(a, b)$, there exists the canonical parameter $\tilde{a}$ defined by

$$\tilde{a} = \int_0^a \frac{ds}{w(s)},\ \text{where } w(s) = \left.\frac{\partial\,\phi(s, b)}{\partial b}\right|_{b=0}.$$

1.3 Prolongation of point transformations and Group generator

The derivatives of u with respect to x are defined as

$$u_i^\alpha = D_i(u^\alpha), \quad u_{ij}^\alpha = D_j D_i(u_i), \cdots, \tag{1.3}$$

where

$$D_i = \frac{\partial}{\partial x^i} + u_i^\alpha \frac{\partial}{\partial u^\alpha} + u_{ij}^\alpha \frac{\partial}{\partial u_j^\alpha} + \cdots, \quad i = 1, ..., n \tag{1.4}$$

is the operator of total differentiation. The collection of all first derivatives u_i^α is denoted by $u_{(1)}$, i.e.,

$$u_{(1)} = \{u_i^\alpha\} \quad \alpha = 1, ..., m, \quad i = 1, ..., n.$$

Similarly

$$u_{(2)} = \{u_{ij}^\alpha\} \quad \alpha = 1, ..., m, \quad i, j = 1, ..., n$$

and $u_{(3)} = \{u_{ijk}^\alpha\}$ and likewise $u_{(4)}$ etc. Since $u_{ij}^\alpha = u_{ji}^\alpha$, $u_{(2)}$ contains only u_{ij}^α for $i \leq j$. In the same manner $u_{(3)}$ has only terms for $i \leq j \leq k$. There is natural ordering in $u_{(4)}$, $u_{(5)}$ $\cdots$.

In group analysis all variables $x, u, u_{(1)} \cdots$ are considered functionally independent variables connected only by the differential relations (1.3). Thus the u_s^α are called differential variables [12].

We now consider a pth-order PDE(s), namely

$$E_\alpha(x, u, u_{(1)}, ..., u_{(p)}) = 0. \tag{1.5}$$

Prolonged or extended groups

If $z = (x, u)$, one-parameter group of transformations G is

$$\bar{x}^i = f^i(x, u, a), \quad f^i|_{a=0} = x^i,$$

$$\bar{u^\alpha} = \phi^\alpha(x,u,a), \quad \phi^\alpha|_{a=0} = u^\alpha. \tag{1.6}$$

According to the Lie's theory, the construction of the symmetry group G is equivalent to the determination of the corresponding *infinitesimal transformations* :

$$\bar{x^i} \approx x^i + a\,\xi^i(x,u), \quad \bar{u^\alpha} \approx u^\alpha + a\,\eta^\alpha(x,u) \tag{1.7}$$

obtained from (1.1) by expanding the functions f^i and ϕ^α into Taylor series in a about $a = 0$ and also taking into account the initial conditions

$$f^i\big|_{a=0} = x^i, \quad \phi^\alpha|_{a=0} = u^\alpha.$$

Thus, we have

$$\xi^i(x,u) = \frac{\partial f^i}{\partial a}\bigg|_{a=0}, \quad \eta^\alpha(x,u) = \frac{\partial \phi^\alpha}{\partial a}\bigg|_{a=0}. \tag{1.8}$$

One can now introduce the *symbol* of the infinitesimal transformations by writing (1.7) as

$$\bar{x^i} \approx (1 + a\,X)x, \quad \bar{u^\alpha} \approx (1 + a\,X)u,$$

where

$$X = \xi^i(x,u)\frac{\partial}{\partial x^i} + \eta^\alpha(x,u)\frac{\partial}{\partial u^\alpha}. \tag{1.9}$$

This differential operator X is known as the infinitesimal operator or generator of the group G. If the group G is admitted by (1.5), we say that X is an *admitted operator* of (1.5) or X is an *infinitesimal symmetry* of equation (1.5).

We now see how the derivatives are transformed.

The D_i transforms as

$$D_i = D_i(f^j)\bar{D}_j, \tag{1.10}$$

where $\bar{D}_j$ is the total differentiations in transformed variables $\bar{x}^i$. So

$$\bar{u}_i^\alpha = \bar{D}_j(u^\alpha), \qquad \bar{u}_{ij}^\alpha = \bar{D}_j(\bar{u}_i^\alpha) = \bar{D}_i(\bar{u}_j^\alpha), \cdots.$$

Now let us apply (1.10) and (1.6)

$$\begin{aligned} D_i(\phi^\alpha) &= D_i(f^j)\bar{D}_j(\bar{u}^\alpha) \\ &= D_i(f^j)\bar{u}_j^\alpha. \end{aligned} \tag{1.11}$$

Thus

$$\left(\frac{\partial f^j}{\partial x^i} + u_i^\beta \frac{\partial f^j}{\partial u^\beta}\right)\bar{u}_j^\alpha = \frac{\partial \phi^\alpha}{\partial x^i} + u_i^\beta \frac{\partial \phi^\alpha}{\partial u^\beta}. \tag{1.12}$$

The quantities $\bar{u}_j^\alpha$ can be represented as functions of $x, u, u_{(i)}$, a for small a, ie., (1.12) is locally invertible:

$$\bar{u}_i^\alpha = \psi_i^\alpha(x, u, u_{(1)}, a), \quad \psi^\alpha|_{a=0} = u_i^\alpha. \tag{1.13}$$

The transformations in $x, u, u_{(1)}$ space given by (1.6) and (1.13) form a one-parameter group (one can prove this but we do not consider the proof) called the first prolongation or just extension of the group G and denoted by $G^{[1]}$.

We let

$$\bar{u}_i^\alpha \approx u_i^\alpha + a\zeta_i^\alpha \tag{1.14}$$

be the infinitesimal transformation of the first derivatives so that the infinitesimal transformation of the group $G^{[1]}$ is (1.7) and (1.14).

Higher-order prolongations of G, viz. $G^{[2]}$, $G^{[3]}$ can be obtained by derivatives of (1.11).

Prolonged generators

Using (1.11) together with (1.7) and (1.14) we get

$$\begin{aligned}
D_i(f^j)(\bar{u}_j^\alpha) &= D_i(\phi^\alpha) \\
D_i(x^j + a\xi^j)(u_j^\alpha + a\zeta_j^\alpha) &= D_i(u^\alpha + a\eta^\alpha) \\
(\delta_i^j + aD_i\xi^j)(u_j^\alpha + a\zeta_j^\alpha) &= u_i^\alpha + aD_i\eta^\alpha \\
u_i^\alpha + a\zeta_i^\alpha + au_j^\alpha D_i\xi^j &= u_i^\alpha + aD_i\eta^\alpha \\
\zeta_i^\alpha &= D_i(\eta^\alpha) - u_j^\alpha D_i(\xi^j), \quad \text{(sum on } j). \qquad (1.15)
\end{aligned}$$

This is called the first prolongation formula. Likewise, one can obtain the second prolongation, viz.,

$$\zeta_{ij}^\alpha = D_j(\eta_i^\alpha) - u_{ik}^\alpha D_j(\xi^k), \quad \text{(sum on } k). \tag{1.16}$$

By induction (recursively)

$$\zeta^{\alpha}_{i_1,i_2,\ldots,i_p} \;=\; D_{i_p}(\zeta^{\alpha}_{i_1,i_2,\ldots,i_{p-1}}) - u^{\alpha}_{i_1,i_2,\ldots,i_{p-1}\,j} D_{i_p}(\xi^j), \quad \text{(sum on } j). \tag{1.17}$$

The first and higher prolongations of the group G form a group denoted by $G^{[1]}, \cdots, G^{[p]}$. The corresponding prolonged generators are

$$\begin{aligned}
X^{[1]} &= X + \zeta^{\alpha}_i \frac{\partial}{\partial u^{\alpha}_i} \quad \text{(sum on } i, \alpha), \\
&\;\;. \\
&\;\;. \\
&\;\;. \\
X^{[p]} &= X^{[p-1]} + \zeta^{\alpha}_{i_1,\ldots,i_p} \frac{\partial}{\partial u^{\alpha}_{i_1,\ldots,i_p}} \quad p \geq 1,
\end{aligned}$$

where

$$X = \xi^i(x,u)\frac{\partial}{\partial x^i} + \eta^{\alpha}(x,u)\frac{\partial}{\partial u^{\alpha}}.$$

1.3.1 Prolongation of (1+1)-dimensional PDE

Consider a second-order PDE

$$E(t,x,u,u_t,u_x,u_{tt},u_{xx},u_{tx}) = 0, \tag{1.18}$$

where t and x are two independent variables and u is a dependent variable. Let

$$X = \tau(t,x,u)\frac{\partial}{\partial t} + \xi(t,x,u)\frac{\partial}{\partial x} + \eta(t,x,u)\frac{\partial}{\partial u}, \tag{1.19}$$

be the infinitesimal generator of the one-parameter group G of transformation (1.1). The *first prolongation* of the operator X is denoted by $X^{[1]}$ and is given by

$$X^{[1]} = X + \zeta_1(t,x,u,u_t,u_x)\frac{\partial}{\partial u_t} + \zeta_2(t,x,u,u_t,u_x)\frac{\partial}{\partial u_x}$$

where

$$\begin{aligned}
\zeta_1 &= D_t(\eta) - u_t D_t(\tau) - u_x D_t(\xi), \\
\zeta_2 &= D_x(\eta) - u_t D_x(\tau) - u_x D_x(\xi)
\end{aligned}$$

and the total derivatives D_t and D_x are given by

$$D_t = \frac{\partial}{\partial t} + u_t\frac{\partial}{\partial u} + u_{tx}\frac{\partial}{\partial u_x} + u_{tt}\frac{\partial}{\partial u_t} + \cdots\,, \tag{1.20}$$

$$D_x = \frac{\partial}{\partial x} + u_x\frac{\partial}{\partial u} + u_{xx}\frac{\partial}{\partial u_x} + u_{tx}\frac{\partial}{\partial u_t} + \cdots\,. \tag{1.21}$$

Likewise, the the second prolongation of X is given by

$$X^{[2]} = X + \zeta_1\frac{\partial}{\partial u_t} + \zeta_2\frac{\partial}{\partial u_x} + \zeta_{11}\frac{\partial}{\partial u_{tt}} + \zeta_{12}\frac{\partial}{\partial u_{tx}} + \zeta_{22}\frac{\partial}{\partial u_{xx}}. \tag{1.22}$$

where

$$\begin{aligned}
\zeta_{11} &= D_t(\zeta_1) - u_{tt}D_t(\tau) - u_{tx}D_t(\xi),\\
\zeta_{12} &= D_x(\zeta_1) - u_{tt}D_x(\tau) - u_{tx}D_x(\xi),\\
\zeta_{22} &= D_x(\zeta_2) - u_{tx}D_x(\tau) - u_{xx}D_x(\xi).
\end{aligned}$$

Applying the definitions of D_t and D_x given above, we obtain

$$\zeta_1 = \eta_t + u_t\eta_u - u_t\tau_t - u_t^2\tau_u - u_x\xi_t - u_tu_x\xi_u. \tag{1.23}$$

$$\zeta_2 = \eta_x + u_x\eta_u - u_t\tau_x - u_tu_x\tau_u - u_x\xi_x - u_x^2\xi_u. \tag{1.24}$$

$$\begin{aligned}
\zeta_{11} = {}& \eta_{tt} + 2u_t\eta_{tu} + u_{tt}\eta_u + (u_t)^2\eta_{uu} - 2u_{tt}\tau_t - u_t\tau_{tt} - 2(u_t)^2\tau_{tu}\\
&-3u_tu_{tt}\tau_u - (u_t)^3\tau_{uu} - 2u_{tx}\xi_t - u_x\xi_{tt} - 2u_tu_x\xi_{tu} - (u_t)^2u_x\xi_{uu}\\
&-(u_xu_{tt} + 2u_tu_{tx})\xi_u.
\end{aligned} \tag{1.25}$$

$$\begin{aligned}
\zeta_{12} = {}& \eta_{tx} + u_x\eta_{tu} + u_t\eta_{xu} + u_{tx}\eta_u + u_tu_x\eta_{uu} - u_{tx}(\tau_t + \xi_x) - u_t\tau_{tx} - u_{tt}\tau_x\\
&-u_tu_x(\tau_{tu} + \xi_{xu}) - u_t^2\tau_{xu} - (2u_tu_{tx} + u_xu_{tt})\tau_u - (u_t)^2u_x\tau_{uu} - u_x\xi_{tx}\\
&-u_{xx}\xi_t - (u_x)^2\xi_{tu} - (2u_xu_{tx} + u_tu_{xx})\xi_u - u_t(u_x)^2\xi_{uu}.
\end{aligned} \tag{1.26}$$

$$\begin{aligned}
\zeta_{22} = {}& \eta_{xx} + 2u_x\eta_{xu} + u_{xx}\eta_u + (u_x)^2\eta_{uu} - 2u_{xx}\xi_x - u_x\xi_{xx} - 2(u_x)^2\xi_{xu}\\
&-3u_xu_{xx}\xi_u - (u_x)^3\xi_{uu} - 2u_{tx}\tau_x - u_t\tau_{xx}\\
&-2u_tu_x\tau_{xu} - (u_tu_{xx} + 2u_xu_{tx})\tau_u - u_t(u_x)^2\tau_{uu}.
\end{aligned} \tag{1.27}$$

1.4 Group admitted by a PDE

Definition 1.2 The vector field

$$X=\xi^i(x,u)\frac{\partial}{\partial x^i}+\eta^\alpha(x,u)\frac{\partial}{\partial u^\alpha}, \tag{1.28}$$

is a *point symmetry* of the pth-order PDE (1.5), if

$$X^{[p]}(E_\alpha)=0 \tag{1.29}$$

whenever $E_\alpha=0$. This can also be written as

$$X^{[p]}\,E_\alpha\big|_{E_\alpha=0}=0, \tag{1.30}$$

where the symbol $\big|_{E_\alpha=0}$ means evaluated on the equation $E_\alpha=0$.

Definition 1.3 Equation (1.29) is called the *determining equation* of (1.5) because it determines all the infinitesimal symmetries of (1.5).

Definition 1.4 (Symmetry group) A one-parameter group G of transformations (1.1) is called a symmetry group of equation (1.5) if (1.5) is form-invariant (has the same form) in the new variables $\bar{x}$ and $\bar{u}$, i.e.,

$$E_\alpha(\bar{x},\bar{u},\bar{u_{(1)}},\cdots,\bar{u_{(p)}})=0, \tag{1.31}$$

where the function E_α is the same as in equation (1.5).

1.5 Group invariants

Definition 1.5 A function $F(x,u)$ is called an *invariant of the group of transformation* (1.1) if

$$F(\bar{x},\bar{u})\equiv F(f^i(x,u,a),\,\phi^\alpha(x,u,a))=F(x,u), \tag{1.32}$$

identically in x, u and a.

Theorem 1.2 (Infinitesimal criterion of invariance) A necessary and sufficient condition for a function $F(x,u)$ to be an invariant is that

$$X\,F\equiv\xi^i(x,u)\frac{\partial F}{\partial x^i}+\eta^\alpha(x,u)\frac{\partial F}{\partial u^\alpha}=0\,. \tag{1.33}$$

It follows from the above theorem that every one-parameter group of point transformations (1.1) has $n-1$ functionally independent invariants, which can be taken to be the left-hand side of any first integrals

$$J_1(x,u) = c_1, \cdots, J_{n-1}(x,u) = c_n$$

of the characteristic equations

$$\frac{dx^1}{\xi^1(x,u)} = \cdots = \frac{dx^n}{\xi^n(x,u)} = \frac{du^1}{\eta^1(x,u)} = \cdots = \frac{du^n}{\eta^n(x,u)}.$$

Theorem 1.3 If the infinitesimal transformation (1.7) or its symbol X is given, then the corresponding one-parameter group G is obtained by solving the Lie equations

$$\frac{d\bar{x^i}}{da} = \xi^i(\bar{x},\bar{u}), \quad \frac{d\bar{u^\alpha}}{da} = \eta^\alpha(\bar{x},\bar{u}) \tag{1.34}$$

subject to the initial conditions

$$\bar{x^i}\big|_{a=0} = x, \quad \bar{u^\alpha}\big|_{a=0} = u\,.$$

1.6 Lie algebras

Let us consider two operators X_1 and X_2 defined by

$$X_1 = \tau_1(t,x,u)\frac{\partial}{\partial t} + \xi_1(t,x,u)\frac{\partial}{\partial x} + \eta_1(t,x,u)\frac{\partial}{\partial u},$$

and

$$X_2 = \tau_2(t,x,u)\frac{\partial}{\partial t} + \xi_2(t,x,u)\frac{\partial}{\partial x} + \eta_2(t,x,u)\frac{\partial}{\partial u}.$$

Definition 1.6 (Commutator) The *commutator* of X_1 and X_2, written as $[X_1, X_2]$, is defined by $[X_1, X_2] = X_1(X_2) - X_2(X_1)$.

Definition 1.7 (Lie algebra) A Lie algebra is a vector space L of operators with the following property : For all $X_1, X_2 \in L$, the commutator $[X_1, X_2] \in L$.

The dimension of a Lie algebra is the dimension of the vector space L.

Theorem 1.4 The set of all solutions of any determining equation forms a Lie algebra.

1.7 Conclusion

In this chapter, we have given some basic definitions and results of the Lie symmetry analysis of PDEs. These included the algorithm to determine the Lie point symmetries.

Chapter 2

Symmetries analysis of the Burger's equation in fluid dynamics: Illustrative example

In this chapter, we consider a basic partial differential equation from fluid mechanics called Burger's equation. It occurs in various applications, such as modelling of gas dynamics, viscous and turbulence flows to name a few. Lie symmetries of the Burger's equation are calculated and its group-invariant solutions under certain symmetry generators are obtained.

2.1 Lie symmetries of the Burger's equation

Example 2.1 :

We consider the general incompressible Navier-Stokes equation, see [13]

$$\rho(\frac{\partial \mathbf{u}}{\partial t} + \mathbf{u}\cdot \nabla \mathbf{u}) = -\nabla P + \mu \Delta \mathbf{u} + \mathbf{F}, \tag{2.1}$$

where ρ is the fluid density, $\mathbf{u}$ is the velocity of the fluid, P is the pressure, μ is dynamic viscosity and $\mathbf{F}$ is an external body force.

The special case of equation (2.1), by assuming that the flow is unsteady and one-dimensional in space. Also, neglecting the external force and taking pressure gradient to be minimal, the above equation (2.1) becomes a (1+1)-dimensional Navier-Stokes equation (2.1) in time and x-direction, named after Johannes Martinus Burger, which is called the Burger's equation [14] given by

$$u_t + uu_x - \nu u_{xx} = 0, \tag{2.2}$$

where u is the flow velocity, t and x are independent time and space variables respectively.

We now determine the Lie point symmetries of the one-dimensional Burger's equation (2.2) above which admits the one-parameter Lie group of transformations with infinitesimal generator

$$X = \tau(t,x,u)\frac{\partial}{\partial t} + \xi(t,x,u)\frac{\partial}{\partial x} + \eta(t,x,u)\frac{\partial}{\partial u} \tag{2.3}$$

if and only if

$$X^{[2]}(u_t + uu_x - \nu u_{xx})\big|_{\nu u_{xx}=u_t+uu_x} = 0. \tag{2.4}$$

Using the definition of $X^{[2]}$ from chapter one, we get

$$\begin{aligned}
&\Big[\tau(t,x,u)\frac{\partial}{\partial t} + \xi(t,x,u)\frac{\partial}{\partial x} + \eta(t,x,u)\frac{\partial}{\partial u} + \zeta_1\frac{\partial}{\partial u_t} + \zeta_2\frac{\partial}{\partial u_x} + \zeta_{11}\frac{\partial}{\partial u_{tt}}\\
&+\zeta_{12}\frac{\partial}{\partial u_{tx}} + \zeta_{22}\frac{\partial}{\partial u_{xx}}\Big]\Big(u_t + uu_x - \nu u_{xx}\Big)\Big|_{\nu u_{xx}=u_t+uu_x} = 0,
\end{aligned}$$

and this gives

$$\eta(u_x) + \zeta_1(1) + \zeta_2(u) - \zeta_{22}(1)\Big|_{\nu u_{xx}=u_t+uu_x} = 0, \tag{2.5}$$

substituting the values of ζ_1, ζ_2 and ζ_{22} given by (1.23), (1.24) and (1.27) into equation (2.5) and replacing u_{xx} by $u_t - uu_x$, we have

$$\begin{aligned}
&u_x\eta + \eta_t + u_t\eta_u - u_t\tau_t - u_t^2\tau_u - u_x\xi_t - u_tu_x\xi_u + u\eta_x\\
&+uu_x\eta_u + uu_t\tau_x - uu_tu_x\tau_u - uu_x\xi_x - uu_x^2\xi_u - \nu\eta_{xx}\\
&-2\nu u_x\eta_{xu} - u_t\eta_u - uu_x\eta_u\nu u_x^2\eta_{uu} + 2u_t\xi_x + 2uu_x\xi_x\\
&+\nu u_x\xi_{xx} + 2\nu u_x^2\xi_{xu} + 3u_tu_x\xi_u = 3uu_x^2\xi_u + \nu u_x^3\xi_{uu} + 2\nu u_{tx}\tau_x\\
&+\nu u_t\tau_{xx} + 2\nu u_tu_x\tau_{xu} + u_t^2\tau_u + uu_tu_x\tau_u + 2\nu u_xu_{tx}\tau_u + \nu u_tu_x^2\tau_{uu} = 0
\end{aligned} \tag{2.6}$$

where τ, ξ and η depend on t, x and u. Treating t, x, u, u_t, u_x, and u_{tx} as independent variables, yields the following overdetermined system of linear partial differential equations:

$$
\begin{aligned}
u_x u_{tx} &: \tau_u = 0, && (2.7)\\
u_{tx} &: \tau_x = 0, && (2.8)\\
u_t u_x^2 &: \tau_{uu} = 0, && (2.9)\\
u_t u_x &: \xi_u + \nu\tau_{xu} = 0, && (2.10)\\
u_x^3 &: \xi_{uu} = 0, && (2.11)\\
u_x^2 &: 2u\xi_u + \nu 2\xi_{xu} - \nu\eta_{uu} = 0, && (2.12)\\
u_x &: \eta - \xi_t + u\xi_x - 2\nu\eta_{xu} + \nu\xi_{xx} = 0, && (2.13)\\
u_t &: 2\xi_x - \tau_t - u\tau_x + \nu\tau_{xx} = 0, && (2.14)\\
1 &: \eta_t + u\eta_x - \nu\eta_{xx} = 0. && (2.15)
\end{aligned}
$$

From equation (2.9), we get

$$\tau = a(t,x)u + b(t,x), \tag{2.16}$$

where both $a(t,x)$ and $b(t,x)$ are arbitrary functions of t and x. Using the value of τ from equation (2.16) into equations (2.8) and (2.7) respectively, yields

$$\tau = b(t), \tag{2.17}$$

where $b(t)$ is an arbitrary function of t. From equation (2.11), we get

$$\xi = c(t,x)u + d(t,x), \tag{2.18}$$

where $c(t,x)$ and $d(t,x)$ are arbitrary functions of t and x. Substituting the above values of τ and ξ into equation (2.10), yields $c(t,x) = 0$, thus

$$\xi = d(t,x). \tag{2.19}$$

Substituting the above value of ξ from equation (2.19) into equation (2.12) and thereafter solving for η, gives

$$\eta = e(t,x)u + f(t,x), \tag{2.20}$$

where $e(t,x)$ and $f(t,x)$ are arbitrary functions of t and x. Using equations (2.19) and (2.20) in equation (2.13), given

$$e(t,x)u + f(t,x) - d_t(t,x) + ud_x(t,x) - 2\nu e_x(t,x) + \nu d_{xx}(t,x) = 0. \tag{2.21}$$

Equating powers of u from equation (2.21) above, yields the following two equations

$$u \quad : \quad e(t,x) + d_x(t,x) = 0, \tag{2.22}$$

$$u^0 \quad : \quad f(t,x) - d_t(t,x) - 2\nu e_x(t,x) + \nu d_{xx}(t,x) = 0. \tag{2.23}$$

Substituting equation (2.20) into equation (2.15), yields

$$e_t(t,x)u + f_t(t,x) + u^2 e_x(t,x) + u f_x(t,x) - \nu e_{xx}(t,x)u - \nu f_{xx}(t,x) = 0, \tag{2.24}$$

Splitting powers of u from equation (2.24), yields

$$u^2 \quad : \quad e_x(t,x) = 0, \tag{2.25}$$

$$u^1 \quad : \quad e_t(t,x) + f_x(t,x) - \nu e_{xx}(t,x) = 0, \tag{2.26}$$

$$u^0 \quad : \quad f_t(t,x) - \nu f_{xx}(t,x) = 0. \tag{2.27}$$

Integrating equation (2.25) with respect to x, we get e as a function of t only, thus

$$e(t,x) = e(t). \tag{2.28}$$

Substituting (2.28) into (2.22) and integrating the resulting equation, with respect to x, yields

$$d(t,x) = e(t)x + d(t), \tag{2.29}$$

where $d(t)$ is an arbitrary function of t. Similarly using (2.28) into (1.13) and solving the resultant equation we get

$$f(t,x) = -e'(t)x + f(t), \tag{2.30}$$

thus, values of ξ and η, becomes

$$\eta = e(t)u - e'(t)x + f(t), \tag{2.31}$$

$$\xi = e(t)x + d(t). \tag{2.32}$$

Taking (2.30) into (2.27) and solving the resulting equation, gives

$$e''(t)x + f'(t) = 0. \tag{2.33}$$

Separating equation (2.33) on x, yields

$$x \quad : \quad e''(t) = 0, \tag{2.34}$$

$$x^0 \quad : \quad f'(t) = 0. \tag{2.35}$$

Integration (2.34) and (2.35) with respect to t respectively, yields

$$e(t) = A_1 t + A_2, \tag{2.36}$$

$$f(t) = A_3, \tag{2.37}$$

where A_1, A_2 and A_3 are constants of integration. Using the above results in equation (2.29) and solving the resultant equation, gives

$$d(t) = -A_3 t + A_4, \tag{2.38}$$

where A_4 is a constant of integration. Thus, the values of τ, ξ and η are given by

$$\tau = b(t), \tag{2.39}$$

$$\xi = (A_1 t + A_2)x - A_3 t + A_4, \tag{2.40}$$

$$\eta = (A_1 t + A_2)u - A_1 x + A_3. \tag{2.41}$$

Substituting (2.39)-(2.41) into (2.14) and solving the resulting equation, we get

$$b(t) = A_1 t^2 + 2A_2 t + A_6, \tag{2.42}$$

where $A_6 = \dfrac{A_5}{2}$ is a constant. Finally the values of τ, ξ and η are as follows

$$\tau = A_1 t^2 + 2A_2 t + A_6, \tag{2.43}$$

$$\xi = A_1 tx + A_2 x - A_3 t + A_4, \tag{2.44}$$

$$\eta = A_1 tu + A_2 u - A_1 x + A_3. \tag{2.45}$$

Thus the infinitesimal symmetries of the Burgers equation are given by

$$\begin{aligned}
X_1 &= \frac{\partial}{\partial t}, \\
X_2 &= \frac{\partial}{\partial x}, \\
X_3 &= t\frac{\partial}{\partial x} - \frac{\partial}{\partial u}, \\
X_4 &= 2t\frac{\partial}{\partial t} + x\frac{\partial}{\partial x} - u\frac{\partial}{\partial u}, \\
X_5 &= t^2\frac{\partial}{\partial t} + tx\frac{\partial}{\partial x} - (x + tu)\frac{\partial}{\partial u}.
\end{aligned}$$

2.2 Group-invariant solutions of the Burgers equation

A group-invariant solution with respect to a subgroup of the symmetry group is an exact solution which is unchanged by all the transformations G of the subgroup. Invariant solutions are expressed in terms of invariant of the subgroup. The number of independent variables in the reduced system is fewer than the original system. Thus, if an equation is invariant under G, the solution of the original system can be obtained from the reduced system.

The group-invariants solution of the Burgers equation

$$u_t + uu_x = u_{xx}, \tag{2.46}$$

are as follows. **Case 1:** We calculate the invariant solution under the symmetry operator

$$X_1 = \frac{\partial}{\partial t}. \tag{2.47}$$

The characteristic equations associated with the above operator are

$$\frac{dt}{1} = \frac{dx}{0} = \frac{u}{0}, \tag{2.48}$$

which gives two invariants

$$J_1 = x, \quad J_2 = u. \tag{2.49}$$

Thus, $u = f(x)$ is the group-invariant solution and f is an arbitrary function. Substituting u into (2.46), yields

$$f^{''}(x) + f(x)f^{'}(x) = 0,$$

which result into the following solution

$$f(x) = C_1 \tanh\left(\frac{1}{2}C_1 x + C_2\right),$$

where C_1 and C_2 are arbitrary constants. Under X_1, the group-invariant solution of (2.46) is given by

$$u(t,x) = C_1 \tanh\left(\frac{1}{2}C_1 x + C_2\right).$$

Case 2: We consider the symmetry operator

$$X_3 = t\frac{\partial}{\partial x} - \frac{\partial}{\partial u}.$$

Now

$$X_3 J = 0\frac{\partial J}{\partial t} + t\frac{\partial J}{\partial x} - \frac{\partial J}{\partial u} = 0. \tag{2.50}$$

The characteristic equations are

$$\frac{dt}{0} = \frac{dx}{t} = \frac{du}{-1}.$$

Thus, one invariant solution is $J_1 = t$. The other is obtained from the equation

$$\frac{dx}{t} = \frac{du}{-1}$$

and is given by $J_2 = \frac{x}{t} + u$. Consequently, the invariant solution of (2.46) under X_3 is $J_2 = f(J_1)$, i.e.,

$$u = -\frac{x}{t} + f(t), \tag{2.51}$$

where f is an arbitrary function. Substituting (2.51) into equation (2.46), gives

$$\frac{x}{t^2} + f'(t) - \left(-\frac{x}{t} + f(t)\right)\left(-\frac{1}{t}\right) = 0$$

and the second-order PDE (2.46) reduces to the first-order ODE

$$\frac{df}{dt} + \frac{f}{t} = 0.$$

Solving for f, we obtain

$$f(t) = \frac{C_3}{t},$$

where C_3 is an arbitrary constant, hence the invariant solution is given by

$$u(t,x) = -\frac{x}{t} + \frac{C_3}{t}.$$

Case 3: Let us construct an invariant solution under the group of dilations generated by

$$X_4 = 2t\frac{\partial}{\partial t} + x\frac{\partial}{\partial x} - u\frac{\partial}{\partial u}.$$

The characteristic equations

$$\frac{dt}{2t} = \frac{dx}{x} = \frac{du}{-u}$$

provide the two invariants $J_1 = \frac{x}{\sqrt{t}}$ and $J_2 = \sqrt{t}u$. Thus the invariant solution is given by $J_2 = f(J_1)$, i.e.,

$$u = \frac{1}{\sqrt{t}} f(\lambda), \text{where} \quad \lambda = \frac{x}{\sqrt{t}}.$$

Substituting this value of u in (2.46), we obtain

$$f'' + ff' + \frac{1}{2}(\lambda f' + f) = 0.$$

This equation can be written as

$$(f')' + \frac{1}{2}(f^2)' + \frac{1}{2}(\lambda f)' = 0,$$

which on integration, yields

$$f' + \frac{1}{2}f^2 + \frac{1}{2}\lambda f = C_4,$$

where C_4 is an arbitrary constant of integration. If $C_4 = 0$, then one can solve the corresponding Bernoulli's equation for f and obtain

$$f(\lambda) = \frac{2}{\sqrt{\pi}}[\frac{exp(-\frac{\lambda^2}{4})}{C_5 + erf(\frac{\lambda}{2})}],$$

where C_5 is an arbitrary constant and

$$erf(z) = \frac{2}{\pi} \int exp(-s^2) ds$$

is the error function. Thus

$$u(t, x) = \frac{2}{\sqrt{\pi t}} \frac{exp(-\frac{x^2}{4t})}{C_5 + erf(\frac{x}{2\sqrt{t}})}$$

is an invariant solution (2.46) under X_4.

Case 4: Finally, we consider symmetry operator

$$X_5 = t^2 \frac{\partial}{\partial t} + tx \frac{\partial}{\partial x} - (x + tu) \frac{\partial}{\partial u}. \tag{2.52}$$

We construct the group-invariant solution of (2.46) under the above symmetry operator and it is given by

$$u(t, x) = \frac{C_6}{t} \tanh \left[\frac{C_6 x}{2t} + C_7 \right] - \frac{x}{t},$$

with C_6 and C_7 being constants.

2.3 Conclusion

In this chapter, we have looked at an example of a non-linear partial differential equation, namely the Burger's equation which arises from fluid dynamics by calculating its Lie point symmetries. We then obtained invariant solutions under certain symmetry generators.

Chapter 3

Lie symmetry analysis of flow and heat transfer inside a filter chamber

In this chapter, we investigate flow dynamics and heat distribution during filtration process. The flow inside the filter chamber is caused by injecting fluid through permeable walls and pressure difference along the axial direction. Also the chapter studies the natural convection due to temperature effect from the walls.

3.1 Introduction

There are advantages to both industry and mathematics that arise from the application of mathematics to industrial case studies. Various industries have used mathematical models to understand the complicated processes better, to increase profit and to improve production. Hence, it is very important to have mathematical models of different industrial phenomena that symbolize real life events. Most of industrial applications lead to (3+1)-dimensional mathematical models due to the fact that the behaviour of such phenomenon are in space and evolve with time, thus yield complex models. On the other hand, a simpler model can be obtain by careful consideration of the system design that might lead to lower dimension without loss of generality. The design of the system is one of the most important step during modelling process that leads to a realistic model and appropriated boundary condition(s).

The study of Newtonian and non-Newtonian fluid flow have been an active area of interest in the past several decades in relation to heat and mass transfer processes through porous media in commercial and industrial processes. Filtration process is one amongst various phenomena which has application of such mass and heat transfer. During filtration process it is important to study heat transfer which is one of the important factors that transform the state of the fluid from Non-Newtonian to Newtonian. Thus, heat transfer affects the mass in flow (through porous medium) and out flow (permeates) during this process. Due to the latter process, many researchers have studied various models in the past and recent to gain better insight of the dynamics of filtration process. Such studies provide engineers, physicists, etc with theoretical insight information of what to expect from the final product produced during filtration process.

During extraction of oil from underground reservoirs, the oil consists of substances which lead to pollution (contaminations), damage to equipment, inefficient burning and other problems. However, various methods are used during filtration process to remove suspended contaminations from oil for either protection of equipment or to extend the life span of the oil. Some examples of filters which are used to purify oil are magnets and filter media. Flow restriction owing to fine pore size of the filter medium is one of the most common challenges during filtration.

To overcome such flow restriction, it is important to have a system design which produce enough permeates while minimizing blockages of filter pores. In order to produce optimal permeates, the design of the current study is such that magnets are integrated in the system to produce load zone that collects iron, steel particles, etc. Thus, the permeable surface will then filter fewer particles as a result pores will take time to become plugged with particles. The system is such that it filters particles before the fluid is refined and separated, most easily by distillation. It is therefore desirable to formulate a mathematical model which can be used to predict the effects of parameters that arise from the design, dynamics of the flow and heat distribution.

Lot of work have been done to study various parameters which are important to the current case study of a laminar flow driven by fluid injection. Such flows have been the subject of many experimental, theoretical and computational studies. Berman [15] introduced the study of a channel flow by investigating a two-dimensional incompressible viscous laminar flow in a channel with porous walls. The author used regular perturbation method to present the analytical solution of the problem. Thereafter, the research work was done to understand more about the dynamics of the flow in a channel with porous walls for small and large injection or suction such as the works done in references [16–18].

The above mentioned studies did not investigate the effects of expanding or contracting walls of channel, thus led to investigations of deformable channel to understand flow through deformable channel. Due to various applications of flow through deformable channels with permeable walls in sciences and engineering such as the transport of biological fluids through contracting or expanding vessels, filtration in kidneys and lungs, regression of the burning surface in the solid rocket motors, air circulation in respiratory systems and etc. These applications led to research efforts to investigate the flow dynamics inside a deformable channel with permeable walls. Uchida and Aoki [19] studied an unsteady flows in a semi-infinite contracting or expanding pipe. Their study modelled the unsteady blood flow produced by forced contractions or expansions of a valved vein.

Dauenhauer and Majdalani [20] considered unsteady flows in semi-infinite rectangular channels with porous and uniformly expanding walls. Exact self-similarity solution of the Navier-Stokes equations for a laminar, incompressible and time-dependent flow in a deforming channel with permeable walls was established by Dauenhauer and Majdalani [21]. The study presents exceptional application of the deforming channel in bio-mechanics. Subsequently, Majdalani et al. [22] investigated the flow field in [21] by using double perturbations in permeation Reynolds number R and wall dilation rate α to obtain analytical solution. Boutros et al. [2] further studied the flow in [21, 22] for slowly expanding or contracting walls with weak permeability. They used Lie-group method to present the similarity transformation of the problem. The difference between [2] and [22] is the transformation technique used to transform partial differential equations representing the flow to ordinary differential equations. Both studies applied double perturbation technique to obtain analytical solutions.

The above mentioned works have studied laminar flow in a deformable channel with permeable walls without taking into consideration forces affecting the flow. Porous media and permeability generate an internal pressure due to the change in momentum (surface force) of the fluid, thus these forces are of great interest in many applications, such as petroleum reservoirs, flows through tobacco rods, pollutant dispersion in aquifers and foam metals, to name a few [23,24]. Porous media plays an important role during filtration process to decrease contaminations and filter particles of a size which are bigger than the pore size.

M. Mahmood et al. [25] extended the model in [22] by taking into consideration the effect of surface forces on the flow field. Authors investigated effect of wall dilation caused by deformable walls, injection or suction due to permeability of the walls and porosity which is due the porous nature of the medium. They used homotopy perturbation and shooting method to find analytical and numerical solutions respectively. Authors observed that the increase in the permeability of medium decreases the axial-velocity of the fluid at the centre of the channel. The results found to be in good agreement with existing non-porous results when the permeability of the medium is zero.

The subject of fluid flow through porous media influenced by magnetic field represents an important area of rapid growth in the present heat transfer research. Hence, heat transfer flow through porous medium has attract considerable attention and has been motivated by a broad range of engineering applications. In relation to these applications, the work of many researchers have studied different system designs to investigate the influence of magnetic field, Joule heating due to magnetic effects, radiation and buoyancy, for more information the reader is referred to [3,26–37].

Sheikholeslami et al. [38] conducted a numerical simulation for two-phase unsteady nanofluid flow and heat transfer between parallel plates in the presence of time-dependent magnetic field. They found out that since magnetic field is applied in the normal direction it brings the so called Lorentz force, which acts against the flow and slows down the fluid velocity. Authors also showed that the absolute values of skin friction coefficient have reverse relationship with the squeeze number and Hartmann number. Sheikholeslami et al. [39] investigated a three-dimensional nanofluid flow between two horizontal parallel rotating plates. The study found that the thermal boundary layer thickness increases when the magnetic parameter increases. Also velocity decreases with increase of magnetic parameter, which is in agreement with results found in [38].

Sharma and Sinha [40] studied an unsteady MHD flow and heat transfer of a fluid over a stretching sheet through porous medium in the presence of viscous dissipation and Joule heating. Their study found that temperature of the fluid increases by increasing radiation parameter, thus fluid particles consume the radiated heat from the heated sheet. Authors also showed that the effect of heat source and dissipation parameter are important to increase the rate of energy transport to the fluid, hence results in increasing fluid temperature and decreasing Nusselt number. Balamurugan et al. [41] studied MHD free convection chemically reactive and radiative flow and heat transfer in a moving inclined porous plate. Authors discussed the effects of radiation, viscous and Joules dissipation on the flow field and heat distribution. They found that the increase in radiation parameter lead to the decrease in temperature and the increase in velocity.

The study to analyse the effects of Joules heating and radiation absorbtion on MHD convective and chemically reactive flow past an inclined porous plate in the presence of heat source and thermal diffusion was conducted by Vijaykumar and Keshava Reddy [42]. Authors used similarity transformation to transform the non-linear partial differential equations governing the fluid flow into a two-point boundary value problem and applied the fourth order Runge-Kutta method with shooting technique to obtain numerical solution. The study showed that by increasing the values of Grashof number, porosity and radiation absorption parameter lead to an increase in fluid velocity but in the case of increasing values of magnetic field and angle of inclination reverse tendency is experienced. Also fluid temperature increases with the increase in values of Prandtl number. Thermal radiation is one of the important factors when the system is operating at high temperature. During operation, the fluid absorbs and emits thermal radiation, thus it is very important to study effect of thermal radiation on the system.

In this project, Lie symmetry analysis [2, 4, 6–12, 43, 44, 53] is used to solve a problem which represents internal flow and heat transfer during filtration process. The main advantage of symmetry analysis method is that it can successfully be applied to non-linear differential equations. The Lie symmetries of differential equations are continuous groups of transformations which leaves the equations invariant under such transformations. The symmetries are quite popular because they result in the reduction of the number of independent variables of the problem. Thereafter, an approximate-analytical solutions for the velocity and temperature profiles are obtained using double perturbation method [45].

The study of flow and heat transfer of an incompressible laminar and viscous fluid in a rectangular domain bounded by porous walls with minimal buoyancy effects was conducted by [7]. The authors studied the effects of various physical parameters affecting the self-axial velocity both analytically and numerically. Also the study found that effects of buoyancy becomes minimal when temperature is constant throughout the system.

The current case study, seeks to find the approximate-analytical solutions of the model representing the above phenomena, thus study equations of continuity, momentum and energy. The resulting flow representing the above mentioned phenomena may be treated as two-dimensional incompressible, viscous and magneto-hydrodynamic (MHD) flow in an inclined porous channel with two walls of weak permeability in the presence of a uniform magnetic field and heat transfer. The nature of porous medium and permeable walls have an influence on fluid flow hence it important to study the effects of permeability and porosity. Motivated by the above mentioned works, the purpose of this study is to generalize the flow analysis of Magalakwe and Khalique [7] in four ways by taking into consideration various forces affecting flow field during filtration process. The first direction is concerned with the influence of a constant magnetic field on the fluid flow while the second investigates the effect of an inclined porous channel on the axial-velocity. Thirdly, the effect of Joule heating due to the presence of uniform magnetic field on an electrically conducting fluid is investigated. Lastly, effects of heat transfer (Thermal radiation) are taken into consideration.

3.2 Mathematical formulation

In this section, we derive set of differential equations representing the internal flow and heat distribution inside an inclined porous channel during filtration process. The mathematical representation of the above mentioned phenomenon is derived in detail using conservation laws of mass, momentum and energy. Forces affecting flow dynamics and heat transfer are also derived based on physical laws such as Darcy's law, Lorenz's law and Fourier's law.

3.2.1 Flow configuration

A two-dimensional, magneto-hydrodynamic (MHD), laminar flow of a viscous incompressible electrically conducting and radiating fluid in an inclined porous filter channel influenced by magnetic field with uniform strength B_0 is considered as shown in **figure 3.1** below. One end of the filter chamber is open and other end is closed with a solid insulated wall while the top and the bottom pearmeable walls are kept at a uniform temperature T_w. The walls allow fluid injection inside the filter chamber or fluid suction out of the filter chamber. The chamber is such that it can uniformly expand or contract at a time dependent rate $\dot{h}(t)$. The fluid emits radiation as soon as the fluid enters the filter chamber with a uniform normal velocity V_w at the walls. The length of the walls are assumed to be infinitely longer than the distance between them. The parallel walls are located at a distance $y = h(t)$ and $y = -h(t)$ from the center of the filter chamber.

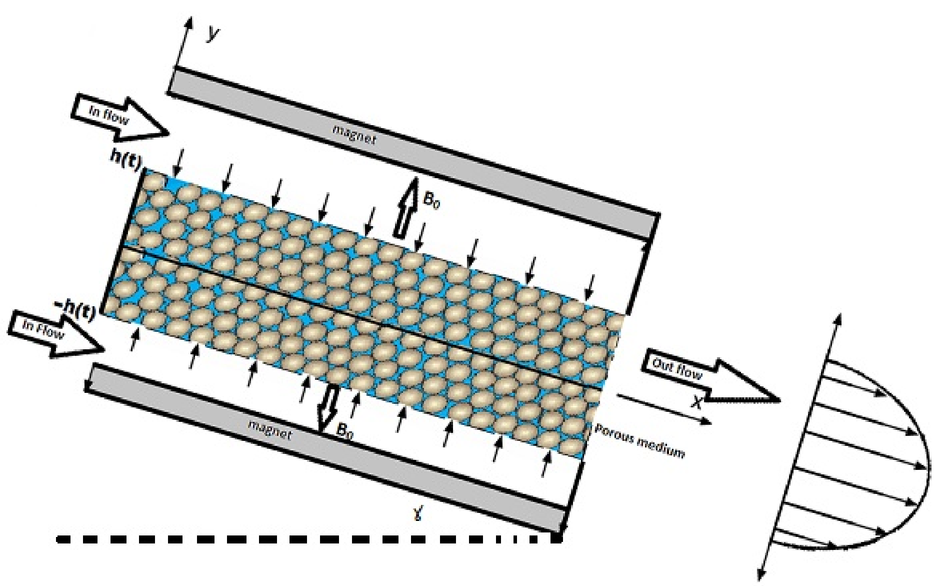

Figure 3.1: Physical model of a filter chamber in the x and y coordinates inclined at angle γ. Note: For this configuration, the symmetric nature of flow is taken into account at y=0.

The system design is such that there is no flow (no fluid injection) in the direction perpendicular to the x-y plane, thus the flow is two-dimensional.

3.2.2 Derivation of equations representing internal flow and heat distribution during filtration process

The mathematical formulation of the internal flow and heat distribution during filtration process is represented by equations derived below. The equations representing the above phenomenon are derived from basic conservation laws such as mass, momentum and energy. Appropriate boundary conditions are formulated based on the filter design, the internal flow dynamics and heat transfer dynamics.

Conservation of mass inside the filter chamber

To have a balanced system, the amount of inflow and outflow through boundaries together with the change of fluid mass in a system must be in balance. That is, the rate of change of fluid mass in a system remains constant, this is known as conservation of mass, which is given by the following equation in Einstein tensor notation [13]

$$\frac{\partial \rho}{\partial t} + \frac{\partial(\rho.u_k)}{\partial x_k} = 0, \tag{3.1}$$

where $k = 1, 2$ and 3 represents the x, y and z directions of flow respectively.

The flow under investigation is considered to be a two-dimensional, along the x and y directions and incompressible, thus equation (3.1) becomes

$$\frac{\partial u}{\partial x} + \frac{\partial v}{\partial y} = 0, \tag{3.2}$$

for $k = 1$ and 2.

Conservation of momentum inside the filter chamber

Inside the filtration chamber (control volume), any rate of change in the momentum of a fluid mass within the chamber is due to the action of external forces on the fluid within the chamber. This rate of change of momentum of a fluid mass in a chamber is equal to the net external forces acting on the fluid mass [13] and this is called conservation of momentum. The external forces acting on a fluid mass are classified as surface forces and body forces. Surface forces act across the surface of the fluid mass, examples of such forces are pressure and viscosity forces. Body forces act throughout the body of the fluid which are gravitational, centrifugal and electromagnetic forces. The conservation of momentum equation is given by the following Naiver-Stokes equation in Einstein tensor notation:

$$\rho\left(\frac{\partial u_i}{\partial t}+u_i\frac{\partial u_j}{\partial x_j}\right)=-\frac{\partial P}{\partial x_i}+\frac{\partial}{\partial x_j}\left(\mu\frac{\partial u_i}{\partial x_j}\right)+F_i, \tag{3.3}$$

where the subscript i and j are used to denote the components of the velocity vector and F_i represent the resultant external force. P is the total pressure given by

$$P=P_w+P_m, \tag{3.4}$$

where P_w is the pressure created by the chamber walls and P_m is the pressure created by the medium. Using (3.4) into (3.3), we have

$$\rho\left(\frac{\partial u_i}{\partial t}+u_i\frac{\partial u_j}{\partial x_j}\right)=-\frac{\partial P_w}{\partial x_i}-\frac{\partial P_m}{\partial x_i}+\frac{\partial}{\partial x_j}\left(\mu\frac{\partial u_i}{\partial x_j}\right)+F_i. \tag{3.5}$$

The total pressure at the chamber wall is given by the following equation (Bernoulli) at the wall and a point inside the filter chamber along the same streamline [13]

$$P_w=p+\rho_w g_i h, \tag{3.6}$$

where p is fluid pressure and $\rho_w g_i h$ is the pressure due to weight of the fluid. Substituting (3.6) into (3.5), we get

$$\rho\left(\frac{\partial u_i}{\partial t}+u_i\frac{\partial u_j}{\partial x_j}\right)=-\frac{\partial p}{\partial x_i}-\frac{\partial \rho_w g_i h}{\partial x_i}-\frac{\partial P_m}{\partial x_i}+\frac{\partial}{\partial x_j}\left(\mu\frac{\partial u_i}{\partial x_j}\right)+F_i, \tag{3.7}$$

which reduces to

$$\rho\left(\frac{\partial u_i}{\partial t}+u_i\frac{\partial u_j}{\partial x_j}\right)=-\frac{\partial p}{\partial x_i}-\rho_w g_i-\frac{\partial P_m}{\partial x_i}+\frac{\partial}{\partial x_j}\left(\mu\frac{\partial u_i}{\partial x_j}\right)+F_i. \tag{3.8}$$

Since

$$\frac{\partial h}{\partial x_i}=1.$$

The above result is due the fact that variation of chamber volume changes with respect to y only. The fluid flow under consideration is influenced by the gravitational force g_i acting on the fluid mass and the electromagnetic force F_{ei}. Therefore, the net external body force acting on a fluid mass is given by

$$F_i = g_i + F_{ei}. \tag{3.9}$$

Substituting (3.9) into (3.8), yields

$$\rho\left(\frac{\partial u_i}{\partial t} + u_i\frac{\partial u_j}{\partial x_j}\right) = -\frac{\partial p}{\partial x_i} - \rho_w g_i + \frac{\partial P_m}{\partial x_i} + \frac{\partial}{\partial x_j}\left(\mu\frac{\partial u_i}{\partial x_j}\right) + \rho g_i + \rho F_{ei}, \tag{3.10}$$

which can be simplified as follows

$$\rho\left(\frac{\partial u_i}{\partial t} + u_i\frac{\partial u_j}{\partial x_j}\right) = -\frac{\partial p}{\partial x_i} - \frac{\partial P_m}{\partial x_i} + \frac{\partial}{\partial x_j}\left(\mu\frac{\partial u_i}{\partial x_j}\right) - (\rho_w - \rho)g_i + \rho F_{ei}. \tag{3.11}$$

According to the design, the flow is unsteady two-dimensional in the x-y plane, thus we have the following momentum equations

$$\frac{\partial u}{\partial t} + u\frac{\partial u}{\partial x} + v\frac{\partial u}{\partial y} = -\frac{1}{\rho}\frac{\partial p}{\partial x} + \nu\left[\frac{\partial^2 u}{\partial x^2} + \frac{\partial^2 u}{\partial y^2}\right] - \frac{\partial P_m}{\partial x} - (\rho_w - \rho)g_x + \rho F_{ex}, \tag{3.12}$$

$$\frac{\partial v}{\partial t} + u\frac{\partial v}{\partial x} + v\frac{\partial v}{\partial y} = -\frac{1}{\rho}\frac{\partial p}{\partial y} + \nu\left[\frac{\partial^2 v}{\partial x^2} + \frac{\partial^2 v}{\partial y^2}\right] - \frac{\partial P_m}{\partial y} - (\rho_w - \rho)g_y + \rho F_{ey}. \tag{3.13}$$

Since there is no density variation and gravitational force along the x-axis. Also, magnetic field is applied normal to the walls producing a Lorentz force only along the x-axis, thus the above equations become

$$\frac{\partial u}{\partial t} + u\frac{\partial u}{\partial x} + v\frac{\partial u}{\partial y} = -\frac{1}{\rho}\frac{\partial p}{\partial x} + \nu\left[\frac{\partial^2 u}{\partial x^2} + \frac{\partial^2 u}{\partial y^2}\right] - \frac{\partial P_m}{\partial x} + \rho F_{ex}, \tag{3.14}$$

$$\frac{\partial v}{\partial t} + u\frac{\partial v}{\partial x} + v\frac{\partial v}{\partial y} = -\frac{1}{\rho}\frac{\partial p}{\partial y} + \nu\left[\frac{\partial^2 v}{\partial x^2} + \frac{\partial^2 v}{\partial y^2}\right] - \frac{\partial P_m}{\partial y} - (\rho_w - \rho)g_y. \tag{3.15}$$

Now, we construct the forces affecting momentum in detail.

Surface force: Porosity

Flow in a porous medium can be understood by examining Darcy's law. Darcy's law is a generalized relationship for flow in porous medium and it represents fluid flow through porous medium. The law was formulated by Henry Darcy as a result of his experiments on the flow of water through sand beds. Darcy discovered that the volumetric flow rate of the fluid is dependant on number of variables namely, the flow area through which the fluid is flowing, elevation, fluid pressure/hydraulic head and a proportionality constant.

Thus, the mathematical representation of Darcy's law is

$$Q = AK\frac{\Delta h}{\Delta L}, \tag{3.16}$$

where Q is volumetric flow rate, A is the flow area perpendicular to the flow path L, K is the hydraulic conductivity (proportionality constant) and h is the hydraulic head. The hydraulic head h at a specific point is the sum of the pressure head and the elevation z given by the following equation:

$$h = \frac{P_m}{\rho g} + z, \tag{3.17}$$

where P_m is the fluid pressure created by the medium, ρ is the fluid density, g is the gravitational acceleration and z is the elevation. For the problem at hand there is no change in elevation between any two points within the filter chamber (fully developed) and it follows that $z = 0$. Taking into account that the flow is incompressible, Darcy's law in differential form takes the form

$$Q = -AK\frac{d}{dL}\left(\frac{P_m}{\rho g}\right). \tag{3.18}$$

The negative sign accounts for the known fact that a fluid flows from a region of high to low pressure. We also note that the velocity and flux equations are given by

$$\mathbf{u} = \frac{\mathbf{q}}{\phi}, \tag{3.19}$$

$$\mathbf{q} = \frac{Q}{A}, \tag{3.20}$$

where ϕ is the porosity of the medium and $\mathbf{q}$ is the Darcy flux. Substituting equations (3.19) and (3.20) into equation (3.18) and making pressure gradient the subject of the formula yields

$$\frac{\partial P_m}{\partial L} = -\frac{\phi \rho g}{K}\mathbf{u}. \tag{3.21}$$

The conductivity K can be replaced by the permeability of the media. The two properties are related by the following equation:

$$K = \frac{k\rho g}{\nu}, \tag{3.22}$$

such that

$$\frac{\partial P_m}{\partial L} = -\frac{\nu\phi}{k}\mathbf{u}, \tag{3.23}$$

where k is the permeability, ν is the fluid kinetic viscosity and $\mathbf{u}$ is the velocity vector. Since L is the flow path and the problem under investigation is two-dimensional, along the x-y directions. Thus (3.23) yields two surface forces in x and y directions as

$$\frac{\partial P_m}{\partial x} = -\frac{\nu\phi}{k}u \qquad \text{and} \qquad \frac{\partial P_m}{\partial y} = -\frac{\nu\phi}{k}v. \tag{3.24}$$

Since the flow under investigation is a pressure driven flow, number of deductions can be made from equation (3.24) based on work and energy principle. The pressure difference in the y-direction is constant since the work done on the surface by fluid is constant due to constant injection. The symmetric nature of the configuration results in no driving force along the y-direction. Also the pressure gradient along the axial direction yields a driving force towards the right, since the work done by the wall on the left side (closed) is more that the work done on right (open). The pressure is force per area, since the system has a closed area on the left only, the pressure on the left is more than the atmospheric pressure on the right (open). Thus, the filtrates outflow is towards the right.

Body force: Buoyancy

Flow between the chamber walls has net force (the difference between the buoyancy and gravity) acting on a unit volume of the fluid inside the boundary layers and it is always in the vertical direction, thus, the net force [46] is given by

$$\mathbf{F}_n = g(\rho_w - \rho), \tag{3.25}$$

where g is gravity, ρ_w is density of the fluid at the wall (at the boundary layer) and ρ is the density of the fluid inside the boundary layer.

Since the filter chamber is inclined the force given by equation (3.25) can be resolved in two components along the x-y directions as follows

$$F_x = \mathbf{F_n}\sin(\gamma) \tag{3.26}$$

which is the force parallel to the walls and force

$$F_y = \mathbf{F_n} \cos(\gamma) \tag{3.27}$$

which is normal to the chamber walls. For the case study under investigation, the density is a function of temperature, hence the density variation of the fluid with temperature at constant pressure can be expressed in terms of the volumetric expansion coefficient β as follows:

$$\beta = -\frac{1}{\rho}\left(\frac{\partial \rho}{\partial T}\right)_P, \tag{3.28}$$

$$\approx -\frac{1}{\rho}\left(\frac{\triangle\, \rho}{\triangle\, T}\right). \tag{3.29}$$

The current flow is incompressible which means the fluid density is constant except in the gravitational term due to Boussinesq approximation [13] which states that for any incompressible fluid that has density variation due temperature difference, density variation can be neglected except along the direction of gravity. Equation (3.29) can be expressed by replacing differential quantities by differences such that

$$\beta \approx -\frac{1}{\rho}\frac{\triangle\, \rho}{\triangle\, T} = -\frac{1}{\rho}\frac{\rho - \rho_w}{T - T_w} \tag{3.30}$$

which can be rewritten as

$$\rho_w - \rho = \rho\beta(T - T_w), \tag{3.31}$$

where T and T_w are fluid temperature and temperature at the boundary layer respectively. Substituting (3.31) into (3.26) and (3.27), yields the buoyancy force in the x and y directions respectively

$$F_x = g\rho\beta(T - T_w)\sin(\gamma) \tag{3.32}$$

and

$$F_y = g\rho\beta(T - T_w)\cos(\gamma). \tag{3.33}$$

Body force: Magnetic field

The fluid under investigation is electrically conducting in the presence of a transverse uniform magnetic field. This flow can be understood by a careful consideration of Lorenz's law of electromagnetism. Lorenz's law describes the electromagnetic force $\mathbf{F_e}$ acting on a moving charged particle. For more information the reader is referred to the following books [47–49]. To illustrate the basic concept describing magneto-hydrodynamics phenomena, we consider an electrically conducting fluid moving with a velocity vector $\mathbf{u}$. A magnetic field $\mathbf{B_{app}}$ is applied perpendicular to the velocity vector as shown in **figure 3.2** below.

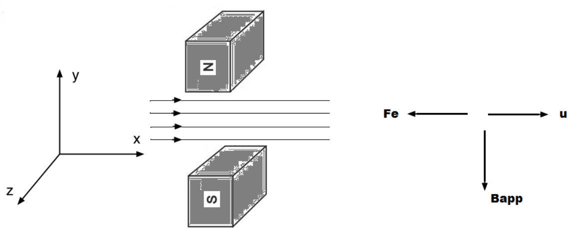

Figure 3.2: Flow of an electrically conducting fluid through magnetic load zone.

A number of deductions can be made from the interaction of the two vector fields. Firstly, an electric field is induced perpendicular to both $\mathbf{u}$ and $\mathbf{B_{app}}$. This electric field, denoted by $\mathbf{E_{ind}}$, is formulated as Ohm's law given by

$$\mathbf{E_{ind}} = \mathbf{u} \times \mathbf{B_{app}}. \tag{3.34}$$

Secondly, a current is induced in the fluid. That is, the positive and the negative charges comprising the fluid are each accelerated in such a way that their average motion gives rise to an electric current, the current density is denoted by $\mathbf{J}$ and is given by

$$\mathbf{J} = \sigma(\mathbf{u} \times \mathbf{B}). \tag{3.35}$$

Here σ is the electrical conductivity of the fluid and $\mathbf{B}$ is the total magnetic field. The magnetic field ($\mathbf{B_{ind}}$) is induced as a result of the induced current ($\mathbf{J}$). That is, intrinsic to a current flowing through a medium (a fluid in our case) is a magnetic field. Thus the total magnetic field in the filter chamber is given by the sum of the applied magnetic field ($\mathbf{B_{app}}$) and the induced magnetic field ($\mathbf{B_{ind}}$), given by

$$\mathbf{B} = (\mathbf{B_{app}} + \mathbf{B_{ind}}). \tag{3.36}$$

Using the result from (3.36), equation (3.35) becomes

$$\mathbf{J} = \sigma[\mathbf{u} \times (\mathbf{B_{app}} + \mathbf{B_{ind}})]. \tag{3.37}$$

Simultaneously occurring with the induced current $\mathbf{J}$, is the induced electromagnetic force or the so called Lorentz force denoted by $\mathbf{F_e}$, given by

$$\mathbf{F_e} = \mathbf{J} \times \mathbf{B}. \tag{3.38}$$

The Lorentz force occurs because the conducting fluid which gives rise to a current perpendicular to the magnetic field. The vector $\mathbf{F_e}$ is the cross product of vectors $\mathbf{J}$ and $\mathbf{B}$ and is perpendicular to the plane of both $\mathbf{J}$ and $\mathbf{B}$. In the current case study, the induced magnetic field is assumed to be small in comparison to the applied magnetic field, i.e. ($\mathbf{B_{app}} >> \mathbf{B_{ind}}$), thus its effect is negligible. Hence, equation (3.37) reduces to

$$\mathbf{J} = \sigma(\mathbf{u} \times \mathbf{B_{app}}). \tag{3.39}$$

For this case study, the MHD fluid is moving with a velocity u along the x-axis, thus

$$\mathbf{u} = u\mathbf{i} \tag{3.40}$$

and the magnetic field acts perpendicular to the direction of fluid flow, which gives

$$\mathbf{B} = B_0\mathbf{j}. \tag{3.41}$$

Substituting equation (3.40) and equation (3.41) into (3.39), gives a current density along the z-axis given by

$$\mathbf{J} = \sigma u B_0 \mathbf{k}. \tag{3.42}$$

Also substituting (3.41) and (3.42) into (3.38), yields the Lorentz force acting along the negative x-axis as

$$\mathbf{F_e} = -\sigma u B_0^2 \mathbf{i}. \tag{3.43}$$

Therefore, the Lorentz force induced by the interaction of the axial-velocity u and the transverse magnetic field act opposite to the axial-velocity. The electromagnetic force acts as a drag force. We note that a change in the direction of the magnetic field or the velocity changes the Lorenz's force (3.43) into a flow propelling force.

Substituting the above surface forces (3.24) and body forces (3.33) and (3.43) into the momentum equations (3.14) and (3.15) respectively, yields

$$\frac{\partial u}{\partial t}+u\frac{\partial u}{\partial x}+v\frac{\partial u}{\partial y}=-\frac{1}{\rho}\frac{\partial p}{\partial x}+\nu\left[\frac{\partial^2 u}{\partial x^2}+\frac{\partial^2 u}{\partial y^2}\right]-\frac{\nu\phi}{k}u-\frac{\sigma B_0^2}{\rho}u, \tag{3.44}$$

$$\frac{\partial v}{\partial t}+u\frac{\partial v}{\partial x}+v\frac{\partial v}{\partial y}=-\frac{1}{\rho}\frac{\partial p}{\partial y}+\nu\left[\frac{\partial^2 v}{\partial x^2}+\frac{\partial^2 v}{\partial y^2}\right]-\frac{\nu\phi}{k}v+g\beta(T-T_w)\cos\gamma. \tag{3.45}$$

Conservation of energy inside the filter chamber

Law of conservation of energy state that the rate of storage plus rate of transport of total energy in the control volume (filter chamber) must be balanced by the rate of work done inside the filter chamber and heat transfer to the filter chamber. The differential equation representing incompressible fluid energy transport is as follows

$$\rho\left(\frac{\partial e}{\partial t}+\mathbf{u}\cdot\nabla e\right)=-\nabla\cdot\mathbf{q}+\mu\Phi+Q, \tag{3.46}$$

where e is the internal energy, $\mathbf{u}$ is the velocity vector, $\mathbf{q}$ is the total heat flux vector, Φ is the dissipation function and Q is the heat generated (such as energy generated by electromagnetic). For more information the reader is referred to [50].

The heat flux term in equation (3.46), is given by

$$\mathbf{q}=\mathbf{q_c}+\mathbf{q_r}, \tag{3.47}$$

where $\mathbf{q_c}$ is the heat conduction and $\mathbf{q_r}$ is the radiative heat flux respectively.

The change in energy can be represented in terms of the change in temperature [51] as

$$de=c_p dT, \tag{3.48}$$

where c_p is specific heat capacity.

By using Fourier's law [51] for heat conduction, equation (3.47) can be written as

$$\mathbf{q}=\mathbf{q_c}+\mathbf{q_r}=-k\nabla T+\mathbf{q_r}. \tag{3.49}$$

Using equations (3.48) and (3.49) in equation (3.46), yields

$$\rho c_p\left(\frac{\partial T}{\partial t}+\mathbf{u}\cdot\nabla T\right)=\nabla\cdot(k\nabla T)+\mu\Phi+Q-\nabla\cdot\mathbf{q_r}. \tag{3.50}$$

For convective heat transfer processes of practical interest, the reversible work and the viscous dissipation are small enough to be neglected, thus we have

$$\rho c_p \left(\frac{\partial T}{\partial t} + \mathbf{u} \cdot \nabla T \right) = \nabla \cdot (k \nabla T) + Q - \nabla \cdot \mathbf{q_r}. \tag{3.51}$$

Since the radiative heat transfer along the x-axis is much small than the one along the y-axis, say $\left(\frac{\partial q_r}{\partial x} \ll \frac{\partial q_r}{\partial y} \right)$. Also the flow is an unsteady two-dimensional, hence, equation (3.51) yields

$$\frac{\partial T}{\partial t} + u \frac{\partial T}{\partial x} + v \frac{\partial T}{\partial y} = \frac{k}{\rho c_p} \left(\frac{\partial^2 T}{\partial x^2} + \frac{\partial^2 T}{\partial y^2} \right) - \frac{1}{\rho c_p} \frac{\partial q_r}{\partial y} + \frac{Q}{\rho c_p}. \tag{3.52}$$

Joule heating

The fluid is electrically conducting in the presence of a transverse uniform magnetic field. Thus, it is taken as the current resistance between the upper wall and the lower wall. When the electric current flows through an electrically conducting fluid, electric energy is converted to heat. This is called Joule heating which can be written as a generalized power equation [52]:

$$P = \mathbf{I V_{ol}}, \tag{3.53}$$

where P is energy dissipated per unit time, $\mathbf{V_{ol}}$ is a vector representing energy dissipated per charged fluid particle passing through the fluid and $\mathbf{I}$ is a vector representing the charged fluid particles passing through fluid per unit time.

From the design of the filter chamber under investigation, the Joule heating is calculated per volume, hence differentiating equation (3.53) with respect to the volume (V), yields power per unit volume as

$$\frac{dP}{dV} = \mathbf{J E_{ind}}. \tag{3.54}$$

Substituting the induced electric field (3.34) into equation (3.54), we get

$$\frac{dP}{dV} = \mathbf{J}(\mathbf{u} \times \mathbf{B}). \tag{3.55}$$

Similarly, substituting (3.40), (3.41) and (3.42) into (3.55), yields

$$\frac{dP}{dV} = \sigma B_0^2 u^2. \tag{3.56}$$

Since producing power per unit volume is the same as internal energy/heat generated Q by electric current through an electrically conducting fluid, the internal work done per unit time inside the filter chamber generates internal energy given by

$$Q = \frac{dP}{dV} = \sigma B_0^2 u^2. \tag{3.57}$$

Finally, equation (3.52) takes the form

$$\frac{\partial T}{\partial t} + u\frac{\partial T}{\partial x} + v\frac{\partial T}{\partial y} = \frac{k}{\rho c_p}\left(\frac{\partial^2 T}{\partial x^2} + \frac{\partial^2 T}{\partial y^2}\right) - \frac{1}{\rho c_p}\frac{\partial q_r}{\partial y} + \frac{\sigma B_0^2}{\rho c_p}u^2, \tag{3.58}$$

which represents heat transfer inside the filter chamber.

Boundary conditions

The boundary conditions according to the flow configuration given in figure 3.1 is as follows. Since the flow is symmetric at $y = 0$, we will show the boundary of the upper section only.

At the upper wall, we have

$$\bar{u} = 0, \quad \bar{v} = -V_w, \quad T = T_w \quad \text{at } \bar{y} = h(t). \tag{3.59}$$

The above conditions at wall are based on the reasons below. There is no movement of the chamber wall in the axial direction, thus $\bar{u} = 0$ at the wall. This is a result owing to the no slip condition at the boundary, that is the fluid layer closest to the wall approximates the axial-velocity of the wall. The normal velocity $\bar{v}$ is given by $-V_w = -A\frac{dh(t)}{dy}$ due to fluid injection through the surface of the permeable wall where A is the injection coefficient. Let it be noted that negating the normal velocity V_w yields suction of the fluid from the surface of the permeable wall. The system is such that the wall is kept at constant temperature $T = T_w$.

At the centre, we have

$$\frac{\partial \bar{u}}{\partial \bar{y}} = 0, \quad \bar{v} = 0, \quad \frac{\partial T}{\partial \bar{y}} = 0 \quad \text{at } \bar{y} = 0. \tag{3.60}$$

The above conditions at the centre of the chamber are due to the symmetric nature of the flow. We can deduce that the axial velocity profile will be parabolic and hence the axial-velocity will be maximum at the centre of the filter chamber, thus $\dfrac{\partial \bar{u}}{\partial \bar{y}} = 0$. Furthermore the normal velocity $\bar{v}$ of the fluid is zero at the centre of the chamber. Since there is no movement of fluid in the y-direction at the centre. The temperature will decrease until it reaches its minimum value at the centre, thus $\dfrac{\partial T}{\partial y} = 0$.

Along the y-axis, we have

$$\bar{u} = 0 \quad \text{at} \quad \bar{x} = 0. \tag{3.61}$$

The chamber is such that the is no inflow at $x = 0$, thus the axial-velocity is zero at $x = 0$.

3.3 Mathematical representation of the case study

The two-dimensional flow of incompressible and electrically conducting viscous fluid in an inclined porous rectangular channel bounded by two permeable walls is represented by the following equations and boundary conditions.

3.3.1 Equations and boundary conditions

Mathematical model representing filtration process flow and heat distribution is given by

$$\frac{\partial \bar{u}}{\partial \bar{x}} + \frac{\partial \bar{v}}{\partial \bar{y}} = 0, \tag{3.62}$$

$$\frac{\partial \bar{u}}{\partial t} + \bar{u}\frac{\partial \bar{u}}{\partial \bar{x}} + \bar{v}\frac{\partial \bar{u}}{\partial \bar{y}} = -\frac{1}{\rho}\frac{\partial \bar{P}}{\partial \bar{x}} + \nu\left[\frac{\partial^2 \bar{u}}{\partial \bar{x}^2} + \frac{\partial^2 \bar{u}}{\partial \bar{y}^2}\right] - \frac{\nu\phi}{k}\bar{u} - \frac{\sigma B_0^2}{\rho}\bar{u}, \tag{3.63}$$

$$\begin{aligned}&\frac{\partial \bar{v}}{\partial t} + \bar{u}\frac{\partial \bar{v}}{\partial \bar{x}} + \bar{v}\frac{\partial \bar{v}}{\partial \bar{y}} = -\frac{1}{\rho}\frac{\partial \bar{P}}{\partial \bar{y}} + \nu\left[\frac{\partial^2 \bar{v}}{\partial \bar{x}^2} + \frac{\partial^2 \bar{v}}{\partial \bar{y}^2}\right] - \frac{\nu\phi}{k}\bar{v}\\ &+g\beta(T - T_h)\cos(\gamma),\end{aligned} \tag{3.64}$$

$$\frac{\partial T}{\partial t} + \bar{u}\frac{\partial T}{\partial \bar{x}} + \bar{v}\frac{\partial T}{\partial \bar{y}} = \frac{\bar{k}}{\rho c_p}\left[\frac{\partial^2 T}{\partial \bar{x}^2} + \frac{\partial^2 T}{\partial \bar{y}^2}\right] - \frac{1}{\rho c_p}\frac{\partial q_r}{\partial \bar{y}} + \frac{\sigma B_0^2}{\rho c_p}\bar{u}^2. \tag{3.65}$$

The appropriate boundary conditions are:

$$\begin{aligned}&\text{(i)} \qquad \bar{u} = 0, \quad \bar{v} = -V_w, \quad T = T_w \quad \text{at } \bar{y} = h(t),\\ &\text{(ii)} \qquad \frac{\partial \bar{u}}{\partial \bar{y}} = 0, \quad \bar{v} = 0, \quad \frac{\partial T}{\partial \bar{y}} = 0 \quad \text{at } \bar{y} = 0,\\ &\text{(iii)} \qquad \bar{u} = 0 \quad \text{at } \bar{x} = 0,\end{aligned} \tag{3.66}$$

3.3.2 Non-dimensional analysis

In this subsection, we introduce dimensionless variables to transform equations (3.62)-(3.65) representing the flow and heat distribution inside the filter chamber and boundary conditions (3.66) to a dimensionless system. The introduction of dimensionless variable decreases number of unknown that the system dynamics depends on.

The introduction of dimensional stream function Ψ in terms of velocity components $\bar{u}$ and $\bar{v}$ is as follows

$$\bar{u} = \frac{\partial \bar{\Psi}}{\partial \bar{y}}, \qquad \bar{v} = -\frac{\partial \bar{\Psi}}{\partial \bar{x}} \tag{3.67}$$

satisfies the continuity equation (3.62).

Scaling the chamber height by introducing the dimensionless coordinate $y = \bar{y}/h(t)$ into equation (3.67), we get

$$\bar{u} = \frac{1}{h}\frac{\partial \bar{\Psi}}{\partial y}, \qquad \bar{v} = -\frac{\partial \bar{\Psi}}{\partial \bar{x}}. \tag{3.68}$$

Substituting the values of $\bar{u}$ and $\bar{v}$ from (3.68) into (3.63)-(3.65), we obtain

$$\frac{1}{h}\bar{\Psi}_{yt} - \frac{\dot{h}}{h^2}\bar{\Psi}_y - \frac{\dot{h}}{h^3}\bar{y}\bar{\Psi}_{yy} + \frac{1}{h^2}\bar{\Psi}_y\bar{\Psi}_{\bar{x}y} - \frac{1}{h}\bar{\Psi}_{\bar{x}}\bar{\Psi}_{y\bar{y}} = -\frac{1}{\rho}\bar{P}_{\bar{x}} + \frac{\nu}{h}[\bar{\Psi}_{\bar{x}\bar{x}y} + \bar{\Psi}_{\bar{y}\bar{y}y}]$$
$$-\frac{\nu\phi}{kh}\bar{\Psi}_y - \frac{\sigma\nu B_0^2}{\rho h}\bar{\Psi}_y, \tag{3.69}$$
$$\frac{\dot{h}}{h^2}\bar{y}\bar{\Psi}_{\bar{x}y} - \bar{\Psi}_{\bar{x}t} - \frac{1}{h}\bar{\Psi}_y\bar{\Psi}_{\bar{x}\bar{x}} + \bar{\Psi}_{\bar{x}}\bar{\Psi}_{\bar{x}\bar{y}} = -\frac{1}{\rho}\bar{P}_{\bar{y}} - \nu[\bar{\Psi}_{\bar{x}\bar{x}\bar{x}} + \bar{\Psi}_{\bar{x}\bar{y}\bar{y}}] + \frac{\nu\phi}{k}\bar{\Psi}_{\bar{x}}$$
$$+g\beta(T - T_h)\cos(\gamma), \tag{3.70}$$
$$\frac{\partial T}{\partial t} + \frac{1}{h}\bar{\Psi}_y\frac{\partial T}{\partial \bar{x}} - \bar{\Psi}_{\bar{x}}\frac{\partial T}{\partial \bar{y}} = \frac{\bar{k}}{\rho c_p}\left[\frac{\partial^2 T}{\partial \bar{x}^2} + \frac{\partial^2 T}{\partial \bar{y}^2}\right] - \frac{1}{\rho c_p}\frac{\partial q_r}{\partial \bar{y}} + \frac{\sigma B_0^2}{\rho c_p h^2}\bar{\Psi}_y^2, \tag{3.71}$$

respectively. The dot in the above equations represents how the filter chamber height changes with time t.

Multiplying momentum equation along axial direction (3.69) by h^3 and momentum equation along the normal direction (3.70) with h^2 respectively, yields

$$h^2\bar{\Psi}_{yt} - \dot{h}h\bar{\Psi}_y - \dot{h}\bar{y}\bar{\Psi}_{yy} + h\bar{\Psi}_y\bar{\Psi}_{\bar{x}y} - h^2\bar{\Psi}_{\bar{x}}\bar{\Psi}_{y\bar{y}} = -\frac{h^3}{\rho}\bar{P}_{\bar{x}} + \nu h^2[\bar{\Psi}_{\bar{x}\bar{x}y} + \bar{\Psi}_{\bar{y}\bar{y}y}]$$

$$-\frac{h^2\nu\phi}{k}\bar{\Psi}_y - \frac{h^2\sigma\nu B_0^2}{\rho}\bar{\Psi}_y, \tag{3.72}$$

$$\dot{h}\bar{y}\bar{\Psi}_{\bar{x}y} - h^2\bar{\Psi}_{\bar{x}t} - h\bar{\Psi}_y\bar{\Psi}_{\bar{x}\bar{x}} + h^2\bar{\Psi}_{\bar{x}}\bar{\Psi}_{\bar{x}\bar{y}} = -\frac{h^2}{\rho}\bar{P}_{\bar{y}} - h^2\nu[\bar{\Psi}_{\bar{x}\bar{x}\bar{x}} + \bar{\Psi}_{\bar{x}\bar{y}\bar{y}}] + \frac{h^2\nu\phi}{k}\bar{\Psi}_{\bar{x}}$$

$$+h^2 g\beta(T - T_h)\cos(\gamma). \tag{3.73}$$

Before constructing dimensionless energy representation, the heat flux equation in (3.71) is firstly represented in terms of temperature. The standard Rosseland approximation of radiative heat flux (energy source) term q_r given by [53]

$$q_r = -\frac{4\sigma_*}{3k_r}\frac{\partial T^4}{\partial y}, \tag{3.74}$$

where σ_* and k_r are the Stefan–Boltzmann constant and mean absorption coefficient respectively. The dynamics of the system is such that the temperature difference inside the fluid chamber is sufficiently small such that T^4 can be expressed as a linear combination of temperature using Taylor's series expansion about T, thus

$$T^4 = T_h^4 + 4T_h^3(T - T_h) + 6T_h^2(T - T_h)^2 + \cdots. \tag{3.75}$$

Neglecting higher order terms beyond the first degree in $(T - T_h)$, gives

$$T^4 \cong 4T_h^3 T - 3T_h^4. \tag{3.76}$$

Substituting (3.76) into (3.74) yields

$$q_r = -\frac{4\sigma_*}{3k_r}\frac{\partial}{\partial y}\left[4T_h^3 T - 3T_h^4\right]. \tag{3.77}$$

Using the above equation (3.77) into energy equation (3.71), yields

$$\frac{\partial T}{\partial t} + \frac{1}{h}\bar{\Psi}_y\frac{\partial T}{\partial \bar{x}} - \bar{\Psi}_{\bar{x}}\frac{\partial T}{\partial \bar{y}} = \frac{\bar{k}}{\rho c_p}\left[\frac{\partial^2 T}{\partial \bar{x}^2} + \frac{\partial^2 T}{\partial \bar{y}^2}\right] + \frac{4\sigma_*}{3c_p k_r\rho}\frac{\partial^2}{\partial y^2}\left[4T_h^3 T - 3T_h^4\right] + \frac{\sigma B_0^2}{\rho c_p h^2}\bar{\Psi}_y^2. \tag{3.78}$$

Substituting dimensionless variables defined below:

$$u = \frac{\bar{u}}{V_w}, \quad v = \frac{\bar{u}}{V_w}, \quad x = \frac{\bar{x}}{h(t)}, \quad y = \frac{\bar{y}}{h(t)}, \quad \Psi = \frac{\bar{\Psi}}{hV_w}, \quad P = \frac{\bar{P}}{\rho V_w^2},$$

$$t = \frac{\bar{t}h}{V_w}, \quad \alpha = \frac{h\dot{h}}{\nu}, \quad \theta = \frac{T - T_h}{T_w - T_h}. \tag{3.79}$$

into (3.72), (3.73) and (3.78), we obtain the following dimensionless system

$$\Psi_{y\bar{t}} + \Psi_y \Psi_{xy} - \Psi_x \Psi_{yy} + P_x - \frac{1}{R_e}[\alpha \Psi_y + \alpha y \Psi_{yy} + \Psi_{xxy} + \Psi_{yyy}] + \frac{1}{K}\Psi_y$$
$$+N\Psi_y = 0, \tag{3.80}$$
$$\Psi_{x\bar{t}} + \Psi_y \Psi_{xx} - \Psi_x \Psi_{xy} - P_y - \frac{1}{R_e}[\alpha y \Psi_{xy} + \Psi_{xyy} + \Psi_{xxx}] + \frac{1}{K}\Psi_x$$
$$+\frac{G_r}{R_e^2}\theta \cos\gamma = 0, \tag{3.81}$$
$$\theta_{\bar{t}} + \Psi_y \theta_x - \Psi_x \theta_y - \frac{1}{P_r R_e}\Big[\theta_{xx} + (1+4R)\theta_{yy}\Big] - J\Psi_y^2 = 0, \tag{3.82}$$

where $\alpha = \dfrac{h\dot{h}}{\nu}$ is the wall dilation rate, $R_e = \dfrac{hV_w}{\nu}$ is the permeation Reynolds number, $K = \dfrac{kV_w}{\nu\phi h}$ is the porosity parameter, $P_r = \frac{\rho C_p \nu}{\bar{k}}$ is the Prandtl number, $R = \frac{4\sigma_r T_h^3}{3k_r \bar{k}}$ is the radiation parameter, $G_r = \frac{hg\beta\theta(T_w - T_h)}{V_w^2}$ is the Grashoff number, $J = \frac{\sigma B_0^2 h V_w}{\rho c_p (T_w - T_h)}$ is the Joule heating parameter and $N = \frac{\sigma \nu h B_0^2}{\rho V_w}$ is the Stuarts number.

Through (3.68) and (3.79), we have

$$u = \frac{\partial \Psi}{\partial y}, \qquad v = -\frac{\partial \Psi}{\partial x}. \tag{3.83}$$

The boundary conditions take the following forms

$$\text{(i)} \qquad \Psi_y = 0, \quad \Psi_x = 1, \quad \theta = 1, \quad \text{at } y = 1,$$
$$\text{(ii)} \qquad \Psi_{yy} = 0, \quad \Psi_x = 0, \quad \theta_y = 0, \quad \text{at } y = 0,$$
$$\text{(iii)} \qquad \Psi_y = 0 \quad \text{at } x = 0. \tag{3.84}$$

3.3.3 Parameters affecting filtration process

The flow and heat distribution inside the filter chamber are influenced by the following dimensionless parameters:

Wall dilation rate

The change in chamber height resulting from expanding or contracting of walls is given by wall dilation rate (α). The dilation rate is positive when the filter chamber expand, negative when the filter chamber contract and zero when the filter chamber volume stays the same. Thus, the magnitude of the dilation rate is given by

$$\alpha = \frac{h\dot{h}}{\nu}. \tag{3.85}$$

Permeation Reynolds number

Reynolds number is defined as the ratio of the inertial to viscous forces of a fluid. This parameter is positive when there is fluid injected inside the filter chamber, negative when the fluid is sucked out of the filter chamber or zero when there is no fluid injection or suction. The magnitude of the Reynolds number is given by

$$R_e = \frac{hV_w}{\nu}. \tag{3.86}$$

Porosity variable

The porosity of the medium (K) is a measure of the medium's ability to allow fluid flow. This parameter takes into account the permeability and porosity of the medium as well as some properties of the fluid flow such as fluid viscosity and velocity. The magnitude of the porosity variable has a bearing on the fluid flow. It is expected that the porous medium allows more free flow as the porosity variable becomes large. The porous medium looses its porous nature (theoretically) as R approaches infinity. Thus, porosity is given by

$$K = \frac{kV_w}{\nu\phi h}. \tag{3.87}$$

which can also be written as

$$K = \frac{kV_{material}V_w}{\nu V_{void}h}, \tag{3.88}$$

where $\phi = \dfrac{V_{void}}{V_{material}}$.

Stuart Number

The Stuart number, also known as the magnetic interaction parameter is defined as the ratio of the electro-magnetic to inertial forces of the fluid. Stuart number is relevant for the flow of electrically conducting fluids and it is given by

$$N = \frac{\sigma \nu h B_0^2}{\rho V_w}. \tag{3.89}$$

It can also be rewritten as

$$N = \frac{\sigma \mu h B_0^2}{V_w}, \tag{3.90}$$

where $\mu = \dfrac{\nu}{\rho}$ is the dynamic viscosity.

Grashof number

The Grashof number represents the ratio between the buoyancy force due to spatial variation in the fluid density (caused by temperature difference) to the restraining force due to the viscosity of the fluid. Thus, the Grashof number is defined as follows

$$G_r = \frac{h\,\beta g\,\theta(T_w - T_h)}{V_w^2}. \tag{3.91}$$

Prandtl number

The Prandtl number is given as the ratio of velocity diffusivity to thermal energy diffusivity defined by

$$P_r = \frac{\rho \nu c_p}{\bar{k}}. \tag{3.92}$$

When the Prandtl number is small that is, $P_r \ll 1$, it means that the heat diffuses quickly compared to velocity (i.e. thermal energy diffusivity dominates). On the other hand, with large Prandtl number, $P_r \gg 1$, the momentum diffusivity dominates the fluid behaviour. The relative thickness of both momentum and thermal energy boundary layers is controlled by the Prandtl number.

Radiation parameter

The radiation parameter is defined as the measure of how the fluid emits or absorbs heat energy in the form of electromagnetic waves. Radiation parameter is given by

$$R = \frac{4\sigma_r T_h^3}{3K_r \bar{k}}. \tag{3.93}$$

Joule heating parameter

The Joule heating parameter is defined as the measure of how the electric current flows through an electrically conducting fluid which transfers electric energy to heat.

$$J = \frac{\sigma B_0^2 h V_w}{\rho c_p (T_w - T_h)}. \tag{3.94}$$

3.4 Solution of the case study

In this section, Lie symmetry analysis is used to find the similarity solutions which leaves the system of partial differential equations (3.80)-(3.82) together with the boundary conditions (3.84) representing the internal flow and heat distribution during filtration process invariant.

3.4.1 Lie symmetry analysis

Consider the one-parameter group of infinitesimal transformations in $(x, y, \bar{t}, \Psi, P, \theta)$ which leaves the dynamics of the phenomenon represented by equations (3.80)-(3.82) and boundary conditions (3.84) unchanged, given by

$$\begin{aligned}
x^* &= x + \varepsilon\xi(x, y, \bar{t}, \Psi, P, \theta) + 0(\varepsilon^2), \\
y^* &= y + \varepsilon\zeta(x, y, \bar{t}, \Psi, P, \theta) + 0(\varepsilon^2), \\
t^* &= \bar{t} + \varepsilon\tau(x, y, \bar{t}, \Psi, P, \theta) + 0(\varepsilon^2), \\
\Psi^* &= \Psi + \varepsilon\eta(x, y, \bar{t}, \Psi, P, \theta) + 0(\varepsilon^2), \\
P^* &= P + \varepsilon\phi(x, y, \bar{t}, \Psi, P, \theta) + 0(\varepsilon^2), \\
\theta^* &= \theta + \varepsilon\psi(x, y, \bar{t}, \Psi, P, \theta) + 0(\varepsilon^2),
\end{aligned} \tag{3.95}$$

where ε is the small group parameter. The symmetry group of equations (3.80)-(3.82) will be generated by the vector field of the form

$$X = \xi\frac{\partial}{\partial x} + \zeta\frac{\partial}{\partial y} + \tau\frac{\partial}{\partial \bar{t}} + \eta\frac{\partial}{\partial \Psi} + \phi\frac{\partial}{\partial P} + \psi\frac{\partial}{\partial \theta}, \tag{3.96}$$

where $\xi, \zeta, \tau, \eta, \phi$ and ψ are functions of t, x, y, Ψ, P and θ.

The solutions $\Psi = \Psi(x,y,\bar{t}),\ P = P(x,y,\bar{t})$ and $\theta = \theta(x,y,\bar{t})$ leave the dynamics of the flow, pressure and heat distribution invariant under the transformation (3.96) if

$$\begin{aligned} \Phi_\Psi &= X\big(\Psi - \Psi(x,y,\bar{t})\big) = 0, \\ \Phi_P &= X\big(P - P(x,y,\bar{t})\big) = 0, \\ \Phi_\theta &= X\big(\theta - \theta(x,y,\bar{t})\big) = 0, \end{aligned} \tag{3.97}$$

where Φ is the transformation which leaves the dynamics of the flow, pressure and heat distribution unchanged.

Letting

$$\begin{aligned} \Delta_1 &= \Psi_{y\bar{t}} + \Psi_y\Psi_{xy} - \Psi_x\Psi_{yy} + P_x - \frac{1}{R_e}[\alpha\Psi_y + \alpha y\Psi_{yy} + \Psi_{xxy} + \Psi_{yyy}] + \frac{1}{K}\Psi_y + N\Psi_y, \\ \Delta_2 &= \Psi_{x\bar{t}} + \Psi_y\Psi_{xx} - \Psi_x\Psi_{xy} - P_y - \frac{1}{R_e}[\alpha y\Psi_{xy} + \Psi_{xyy} + \Psi_{xxx}] + \frac{1}{K}\Psi_x + \frac{G_r}{R_e^2}\theta\cos(\gamma), \\ \Delta_3 &= \theta_{\bar{t}} + \Psi_y\theta_x - \Psi_x\theta_y - \frac{1}{P_rR_e}\Big[\theta_{xx} + (1+4R)\theta_{yy}\Big] - J(\Psi_y)^2, \end{aligned}$$

a vector X is said to be a symmetry generator of equations (3.80)-(3.82) if and only if

$$X^{[3]}(\Delta_j)\big|_{\Delta_j=0} = 0, \quad j = 1,2,3, \tag{3.98}$$

where

$$\begin{aligned} X^{[3]} &= \xi\frac{\partial}{\partial x} + \zeta\frac{\partial}{\partial y} + \tau\frac{\partial}{\partial \bar{t}} + \eta\frac{\partial}{\partial \Psi} + \phi\frac{\partial}{\partial P} + \psi\frac{\partial}{\partial \theta} + \eta^x\frac{\partial}{\partial \Psi_x} + \eta^y\frac{\partial}{\partial \Psi_y} + \phi^x\frac{\partial}{\partial P_x} + \phi^y\frac{\partial}{\partial P_y} \\ &+\psi^x\frac{\partial}{\partial \theta_x} + \psi^y\frac{\partial}{\partial \theta_y} + \psi^{\bar{t}}\frac{\partial}{\partial \theta_{\bar{t}}} + \eta^{xy}\frac{\partial}{\partial \Psi_{xy}} + \eta^{x\bar{t}}\frac{\partial}{\partial \Psi_{x\bar{t}}} + \eta^{y\bar{t}}\frac{\partial}{\partial \Psi_{y\bar{t}}} + \eta^{xx}\frac{\partial}{\partial \Psi_{xx}} + \eta^{yy}\frac{\partial}{\partial \Psi_{yy}} \\ &+\psi^{xx}\frac{\partial}{\partial \theta_{xx}} + \psi^{yy}\frac{\partial}{\partial \theta_{yy}} + \eta^{xxy}\frac{\partial}{\partial \Psi_{xxy}} + \eta^{xyy}\frac{\partial}{\partial \Psi_{xyy}} + \eta^{xxx}\frac{\partial}{\partial \Psi_{xxx}} + \eta^{yyy}\frac{\partial}{\partial \Psi_{yyy}} \end{aligned} \tag{3.99}$$

is called the third prolongation of X.

The total derivatives are introduced by differentiating the dependent variables from (3.95) to investigate the change of fluid flow, pressure and temperature inside the filter chamber with respect to time and space variables, thus

$$\begin{aligned} D_x &= \partial_x + \Psi_x\partial_\Psi + \phi_x\partial_p + \theta_x\partial_\theta + \Psi_{xx}\partial_{\Psi_x} + P_{xx}\partial_{P_x} + \theta_{xx}\partial_{\theta_x} + \Psi_{xy}\partial_{\Psi_y} + \theta_{xy}\partial_{\theta_y} + \cdots, \\ D_y &= \partial_y + \Psi_y\partial_\Psi + P_y\partial_P + \theta_y\partial_\theta + \Psi_{yy}\partial_{\Psi_y} + P_{yy}\partial_{P_y} + \theta_{yy}\partial_{\theta_y} + \Psi_{xy}\partial_{\Psi_x} + \theta_{xy}\partial_{\theta_x} + \cdots, \\ D_{\bar{t}} &= \partial_{\bar{t}} + \Psi_{\bar{t}}\partial_\Psi + P_{\bar{t}}\partial_P + \theta_{\bar{t}}\partial_\theta + \Psi_{\bar{t}\bar{t}}\partial_{\Psi_{\bar{t}}} + P_{\bar{t}\bar{t}}\partial_{P_{\bar{t}}} + \theta_{\bar{t}\bar{t}}\partial_{\theta_{\bar{t}}} + \Psi_{x\bar{t}}\partial_{\Psi_x} + \theta_x\bar{t}\partial_{\theta_x} + \cdots. \end{aligned} \tag{3.100}$$

Since τ, ξ, ζ, η, ϕ and ψ depend only on x, y, Ψ, P and θ by treating the variables t,x, y, Ψ, P, θ and the derivatives of Ψ, P and θ as independent variables. We obtain the following determining equations by separating the resulting equations from (3.98) on derivatives of Ψ, P and θ with aid of Mathematica

$$\tau_\theta = 0, \tag{3.101}$$

$$\tau_P = 0, \tag{3.102}$$

$$\tau_\Psi = 0, \tag{3.103}$$

$$\tau_y = 0, \tag{3.104}$$

$$\tau_x = 0, \tag{3.105}$$

$$\xi_\theta = 0, \tag{3.106}$$

$$\xi_P = 0, \tag{3.107}$$

$$\xi_\Psi = 0, \tag{3.108}$$

$$\xi_y = 0, \tag{3.109}$$

$$\xi_{xx} = 0, \tag{3.110}$$

$$\zeta_\theta = 0, \tag{3.111}$$

$$\zeta_P = 0, \tag{3.112}$$

$$\zeta_\Psi = 0, \tag{3.113}$$

$$\zeta_x = 0, \tag{3.114}$$

$$\zeta_{yy} = 0, \tag{3.115}$$

$$\eta_\theta = 0, \tag{3.116}$$

$$\eta_P = 0, \tag{3.117}$$

$$\eta_{\Psi\Psi} = 0, \tag{3.118}$$

$$\phi_\theta = 0, \tag{3.119}$$

$$\psi_P = 0, \tag{3.120}$$

$$\psi_{\Psi} = 0, \tag{3.121}$$

$$\psi_{y} = 0, \tag{3.122}$$

$$\psi_{\theta\theta} = 0, \tag{3.123}$$

$$\eta_{y\Psi} = 0, \tag{3.124}$$

$$\eta_{x\Psi} = 0, \tag{3.125}$$

$$\xi_x - \zeta_y = 0, \tag{3.126}$$

$$\xi_x - \zeta_y - \eta_{\Psi} = 0, \tag{3.127}$$

$$2\zeta_y - \tau_{\bar{t}} = 0, \tag{3.128}$$

$$3\zeta_y - \xi_x - \eta_{\Psi} + \phi_P = 0, \tag{3.129}$$

$$-\phi_P + \eta_{\Psi} + \zeta_y - \xi_x - \tau_{\bar{t}} = 0, \tag{3.130}$$

$$-\phi_P + \eta_{\Psi} + \zeta_y - \xi_x - \eta_{xy} + \eta_{t\Psi} - \xi_{\bar{t}x} = 0, \tag{3.131}$$

$$-\eta_x - \zeta_{\bar{t}} = 0, \tag{3.132}$$

$$\eta_y - \xi_{\bar{t}} = 0, \tag{3.133}$$

$$\phi_{\Psi} - \eta_{yy} = 0, \tag{3.134}$$

$$P_r R_e \eta_y - 2\psi_{x\theta} - P_r R_e \xi_x = 0, \tag{3.135}$$

$$J\psi_{\theta} - 2J\eta_{\Psi} - 2J\eta_y + \psi_x = 0, \tag{3.136}$$

$$\alpha\zeta + \alpha y \zeta_y + \eta_x + \zeta_{\bar{t}} = 0, \tag{3.137}$$

$$R_e\left(\frac{1}{K} + N - \frac{\alpha}{R_e}\right)\eta_y - \alpha y \eta_{yy} - \eta_{yyy} + \phi_x - \eta_{xxy} + \eta_{\bar{t}y} = 0, \tag{3.138}$$

$$-\psi_{xx} + P_r R_e \psi_{\bar{t}} = 0, \tag{3.139}$$

$$KR_eG_r\cos(\gamma)\Psi - KR_eG_r\theta\cos(\gamma)\phi_P + KR_eG_r\theta\cos(\gamma)\zeta_y$$

$$-KR_e\phi_y + R_e\eta_x - Ky\alpha\eta_{xy} - K\eta_{xyy} - K\eta_{xxx} + \eta_{\bar{t}x} = 0, \tag{3.140}$$

$$\eta_y - \xi_{\bar{t}} = 0, \tag{3.141}$$

$$\eta_{\Psi} + \zeta_y - \xi_x = 0, \tag{3.142}$$

$$\left(\frac{2}{K} + 2N - \frac{2\alpha}{R_e}\right)\zeta_y + \eta_{xy} + \eta_{t\Psi} + \zeta_{\bar{t}y} = 0, \tag{3.143}$$

$$\phi_P - \eta_\Psi + \zeta_y + \xi_x = 0, \tag{3.144}$$

$$\phi_P - \eta_\Psi - \zeta_y + \xi_x = 0, \tag{3.145}$$

$$-\phi_P + 2\eta_\Psi - 2\xi_x = 0, \tag{3.146}$$

$$\phi_P - 2\eta_\Psi + 2\xi_x = 0, \tag{3.147}$$

$$-\alpha\zeta + y\alpha\phi_P - y\alpha\eta_\Psi - R_e\eta_x + y\alpha\xi_x - R_e\zeta_{\bar{t}} \tag{3.148}$$

$$-\phi_\Psi + \eta_{xx} = 0, \tag{3.149}$$

$$\eta_\Psi + \zeta_y - \xi_x = 0, \tag{3.150}$$

$$-\zeta_y + \xi_x = 0, \tag{3.151}$$

$$-\eta_\Psi - \zeta_y + \xi_x = 0, \tag{3.152}$$

$$2\zeta_y - \tau_{\bar{t}} = 0, \tag{3.153}$$

Equations (3.101)-(3.105) imply that

$$\tau = a(\bar{t}), \tag{3.154}$$

where $a(\bar{t})$ is an arbitrary function of $\bar{t}$. From equations (3.106)-(3.110), we have

$$\xi = b(\bar{t})x + c(\bar{t}), \tag{3.155}$$

where both $b(\bar{t})$ and $c(\bar{t})$ are arbitrary functions of $\bar{t}$. It also follows from equations (3.111)-(3.115), that

$$\zeta = d(\bar{t})y + e(\bar{t}), \tag{3.156}$$

where $d(\bar{t})$ and $e(\bar{t})$ are arbitrary functions of $\bar{t}$. From equations (3.116)-(3.118), we have

$$\eta = f(\bar{t}, x, y)\Psi + g(\bar{t}, x, y), \tag{3.157}$$

where both $f(\bar{t}, x, y)$ and $g(\bar{t}, x, y)$ are arbitrary functions of $\bar{t}$, x and y. Equation (3.119) implies that

$$\phi = h(\bar{t}, x, y, \Psi, P), \tag{3.158}$$

where $h(\bar{t}, x, y, \Psi)$ is an arbitrary function of $\bar{t}$, x, y and Ψ. From equations (3.120)-(3.123), we obtain

$$\psi = r(\bar{t}, x)\theta + s(\bar{t}, x), \tag{3.159}$$

where $r(\bar{t}, x)$ and $s(\bar{t}, x)$ are arbitrary functions of t and x. Substituting the expression for η from (3.157) into equation (3.124), thereafter integrating with respect to y, we obtain

$$\eta = f_1(\bar{t}, x)\Psi + g(\bar{t}, x, y), \tag{3.160}$$

where $f = f_1$ now depend on $\bar{t}$ and x. Similarly by substituting equation (3.160) into equation (3.125) and integrating the resulting equation with respect x, yields

$$\eta = f_2(t)\Psi + g(t, x, y), \tag{3.161}$$

here $f_2 = f_1$ becomes a function of $\bar{t}$ only. It follows that using equation (3.155) and equation (3.156) into equation (3.126) and solving the obtained equation, gives

$$b(\bar{t}) = d(\bar{t}). \tag{3.162}$$

Therefore equation (3.155) and equation (3.156), becomes

$$\xi = b(\bar{t})x + c(\bar{t}), \tag{3.163}$$

$$\zeta = b(\bar{t})y + e(\bar{t}). \tag{3.164}$$

Substituting equations (3.163), (3.164) and (3.161) into equation (3.127), gives the solution

$$f_2(\bar{t}) = 0,$$

which reduces equation (3.161) to

$$\eta = g(\bar{t}, x, y). \tag{3.165}$$

Using (3.154) and (3.164) into (3.128), we obtain

$$2b(t) = a'(t). \tag{3.166}$$

Subtituting equations (3.163), (3.164) and (3.165) into (3.129) and integrating the obtained equation with respect to P, yields

$$h = -2b(\bar{t})P + h_1(\bar{t}, x, y, \Psi). \tag{3.167}$$

Using (3.167) into (3.158), gives the value of ϕ as

$$\phi = -2b(\bar{t})P + h_1(\bar{t}, x, y, \Psi). \tag{3.168}$$

Using (3.163), (3.164), (3.165) and (3.168) into (3.130), we get

$$-b(\bar{t}) - a'(\bar{t}) = 0, \tag{3.169}$$

which along with (3.166) equation (3.169), yields

$$a'(\bar{t}) = 0,$$

thus

$$a(\bar{t}) = C_1,$$

hence τ, becomes

$$\tau = C_1, \tag{3.170}$$

where C_1 is an arbitrary constant. Also since

$$a'(\bar{t}) = 0,$$

then $b(\bar{t})$ from equation (3.166), becomes

$$b(\bar{t}) = 0 \tag{3.171}$$

Thus ζ, ξ and ϕ become

$$\xi = c(\bar{t}), \tag{3.172}$$

$$\zeta = e(\bar{t}) \tag{3.173}$$

and

$$\phi = h_1(\bar{t}, x, y, \Psi). \tag{3.174}$$

Now using (3.165), (3.172)-(3.174) into equation (3.131) and integrating the resulting equation with respect to y, we get

$$g_x = g_1(\bar{t}, x). \tag{3.175}$$

using (3.165) and (3.173) into equation (3.132) and integrating the resulting equation with respect to x, we obtain

$$g = -e'(\bar{t})x + g_1(\bar{t}, y). \tag{3.176}$$

Thus equation (3.165) becomes

$$\eta = -e'(\bar{t})x + g_1(\bar{t}, y). \tag{3.177}$$

Subtituting (3.173) and (3.177) into (3.133) and thereafter integrating resulting equation with respect to y, yields

$$\eta = -e'(\bar{t})x + c'(\bar{t})y + g_2(\bar{t}). \tag{3.178}$$

Using (3.174) and (3.178) into (3.134) and solving equation obtained, yields

$$\phi = h_2(\bar{t}, x, y). \tag{3.179}$$

Using the expression for η, ξ and ψ into (3.135) and integrating the resulting equation with respect to x, gives the expression for ψ as

$$\psi = \frac{P_r R_e}{2} c'(\bar{t}) x\theta + r_1(\bar{t})\theta + s(\bar{t}, x). \tag{3.180}$$

From substituting (3.178) and (3.180) into (3.136) and spliting the resulting equation on powers of θ, we get

$$\theta \quad : \quad c'(\bar{t}) = 0, \tag{3.181}$$

$$1 \quad : \quad \frac{JP_r R_e}{2} c'(\bar{t})x + Jr_1(\bar{t}) - 2Jc'(\bar{t}) + s(\bar{t}, x) = 0. \tag{3.182}$$

The above equations respectively gives the following solution

$$c(\bar{t}) = C_2,$$

and

$$s(\bar{t}, x) = -Jr_1(\bar{t})x + s_1(\bar{t}).$$

Thus the expressions for τ, ξ, ζ, η, ϕ and ψ, becomes

$$\tau = C_1, \tag{3.183}$$

$$\xi = C_2, \tag{3.184}$$

$$\zeta = e(\bar{t}), \tag{3.185}$$

$$\eta = -e'(\bar{t})x + g_2(\bar{t}), \tag{3.186}$$

$$\phi = h_2(\bar{t}, x, y), \tag{3.187}$$

$$\psi = r_1(\bar{t})\theta - Jr_1(\bar{t})x + s_1(\bar{t}). \tag{3.188}$$

From using (3.185) and (3.186) into (3.137), we obtain

$$e(\bar{t}) = 0,$$

which implies that its derivative is also equal to zero i.e $e'(\bar{t}) = 0$. Therefore the expressions for ζ and η becomes

$$\zeta = 0 \tag{3.189}$$

and

$$\eta = g_2(\bar{t}). \tag{3.190}$$

Substituting the expressions for η and ϕ into (3.138) and integrating the resulting equation with respect to x, we get ϕ to be

$$\phi = h_3(\bar{t}, y). \tag{3.191}$$

Substituting the expression for ψ into (3.139) and splitting the resulting equation by powers of θ, we get

$$\theta \quad : \quad r_1'(\bar{t}) = 0, \tag{3.192}$$

$$1 \quad : \quad Jr_1'(\bar{t})x + s_1'(\bar{t}) = 0. \tag{3.193}$$

From the above equations, we get that

$$r_1(\bar{t}) = C_3,$$

and

$$s_1(\bar{t}) = C_4,$$

Thus

$$\psi = C_3\theta - JC_3x + C_4. \tag{3.194}$$

Substituting (3.189), (3.190), (3.191) and (3.194) into (3.140) and splitting the resulting equation on powers of θ and solving the two obtained equations, we get that

$$C_3 = 0 \tag{3.195}$$

and

$$h_3 = G_r \cos(\gamma) C_4 y + h_4(\bar{t}). \tag{3.196}$$

Hence, the general solution of equations (3.101)-(3.153) is given by

$$\tau = C_1, \quad \xi = C_2, \quad \zeta = 0, \quad \eta = g_2(\bar{t}), \quad \phi = G_r\cos(\gamma)C_4 y + h_4(\bar{t}), \quad \psi = C_4.$$

The system of equations (3.80)-(3.82) has the following Lie-group point symmetries generated by

$$X_1 = \frac{\partial}{\partial \bar{t}}, \quad X_2 = \frac{\partial}{\partial x}, \quad X_3 = g_2(\bar{t})\frac{\partial}{\partial \Psi}, \quad X_4 = G_r\cos(\gamma)y\frac{\partial}{\partial P} + \frac{\partial}{\partial \theta}, \quad X_5 = h_4(\bar{t})\frac{\partial}{\partial P}.$$

Invariant solution

We now use the Lie symmetries that leave the equations representing the flow field, pressure, heat distribution and boundaries invariant. According to solutions (3.97), the generator X_3, X_4 and X_5 have no invariant solutions. The generators X_2 gives the unsteady state regime solutions of the case study. Whereas the symmetry, X_1 gives the steady state regime of the case study which preserve the steady state dynamics of the system, hence the characteristic $\Phi = (\Phi_\Psi, \Phi_P, \Phi_\theta)$ has the components

$$\Phi_\Psi = -\Psi_{\bar{t}}, \quad \Phi_P = -P_{\bar{t}}, \quad \Phi_\theta = -\theta_{\bar{t}}$$

for steady state operation during filtration process. The general solutions of the above invariant conditions satisfying the boundary conditions are given by

$$\Psi = h(y)H(x,y), \qquad P = \Gamma(x,y), \qquad \theta = \tau(x,y). \tag{3.197}$$

Substituting (3.197) into (3.80), we get

$$\begin{aligned} &h'hHH_{xy} + (h')^2HH_x + h^2H_yH_{xy} - hh'H_xH_y - hh''HH_x - h^2H_xH_{yy} \\ &+\Gamma_x - \tfrac{1}{R_e}\Big(\alpha h'H + \alpha hH_y + \alpha yh''H + 2\alpha yh'H_y + \alpha yhH_{yy} \\ &+h'H_{xx} + hH_{xxy} + h'''H + 3h''H_y + 3h'H_{yy} + hH_{yyy}\Big) \\ &+\tfrac{1}{K}h'H + \tfrac{1}{K}hH_y + Nh'H + NhH_y = 0, \end{aligned} \tag{3.198}$$

which after multiplying by $\frac{1}{H}$, becomes

$$
\begin{aligned}
& h'hH_{xy} + (h')^2 H_x + h^2 \tfrac{H_y H_{xy}}{H} - hh' \tfrac{H_x H_y}{H} - hh'' H_x - h^2 \tfrac{H_x H_{yy}}{H} \\
& + \tfrac{1}{H}\Gamma_x - \tfrac{1}{R_e}\Bigg(\alpha h' + \alpha h \tfrac{H_y}{H} + \alpha y h'' + 2\alpha y h' \tfrac{H_y}{H} + \alpha y h \tfrac{H_{yy}}{H} \\
& + h' \tfrac{H_{xx}}{H} + h \tfrac{H_{xxy}}{H} + h''' + 3h'' \tfrac{H_y}{H} + 3h' \tfrac{H_{yy}}{H} + h \tfrac{H_{yyy}}{H} \Bigg) \\
& + \tfrac{1}{K} h' + \tfrac{1}{K} h \tfrac{H_y}{H} + N h' + N h \tfrac{H_y}{H} = 0. \qquad (3.199)
\end{aligned}
$$

By letting

$$
\begin{aligned}
& B_1 = H_x, \quad B_2 = \frac{H_y}{H}, \quad B_3 = \frac{H_x H_y}{H}, \quad B_4 = H_{xy}, \quad B_5 = \frac{H_{xx}}{H}, \quad B_6 = \frac{H_{yy}}{H}, \\
& B_7 = \frac{H_y H_{xy}}{H}, \quad B_8 = \frac{H_x H_{yy}}{H}, \quad B_9 = \frac{H_{xxy}}{H}, \quad B_{10} = \frac{H_{yyy}}{H}, \quad B = \frac{1}{R_e}. \qquad (3.200)
\end{aligned}
$$

Equation (3.199) in terms of the values given in (3.200) takes the form

$$
\begin{aligned}
& -B \frac{d^3 h}{dy^3} + \Bigg[-\alpha B y - h B_1 - 3 B B_2 \Bigg] \frac{d^2 h}{dy^2} \\
& + \Bigg[-\alpha B - 2\alpha B y B_2 - h B_3 + h B_4 - B B_5 - 3 B B_6 + \frac{1}{K} + N \Bigg] \frac{dh}{dy} \\
& B_1 \Bigg(\frac{dh}{dy} \Bigg)^2 + \Bigg[-\alpha B B_2 + \frac{1}{K} B_2 + N B_2 - \alpha B B_6 y - B B_9 - B B_{10} \Bigg] h \\
& + \Bigg[B_7 - B_8 \Bigg] h^2 + \frac{1}{H} \frac{d\Gamma}{dx} = 0. \qquad (3.201)
\end{aligned}
$$

Integrating $H_x = B_1$ from (3.200), we get the steady state velocity as

$$
H(x, y) = x B_1(y) + B_{11}(y). \qquad (3.202)
$$

Substituting above equation into $\Psi = h(y)H(x, y)$, we obtain dimensionless stream function for steady state regime as

$$
\Psi = [x B_1(y) + B_{11}(y)] h(y). \qquad (3.203)
$$

Differentiating the above dimensionless stream function from equation (3.203) with respect to y and imposing boundary conditions (3.84) (iii), we get

$$
B_{11}(y) h(y) = B_{12}, \qquad (3.204)
$$

where B_{12} is a constant of integration.

Substituting B_{12} into the stream function (3.203), yields

$$\Psi = xG(y) + B_{12}, \tag{3.205}$$

where $G(y) = B_1(y)h(y)$. Substitution of the steady state pressure $P = \Gamma(x, y)$ and (3.202) into momentum equation along x (3.201), yields

$$B_{11} = 0. \tag{3.206}$$

Equation (3.202) when $B_{11} = 0$ becomes

$$H(x, y) = xB_1(y) \tag{3.207}$$

and B_{12} becomes zero from equation (3.204). Using $B_{12} = 0$ from the above results, the dimensionless stream function (3.205) becomes

$$\Psi = xG(y). \tag{3.208}$$

Substituting equation (3.208) into (3.83), yields the axial and normal velocity components as

$$\frac{u}{x} = \frac{dG(y)}{dy}, \qquad v = -G(y), \tag{3.209}$$

for steady state regime. The above results confirms the laminar nature of the flow field inside the filter chamber. It can be noted that the axial-velocity profile is parabolic since the system is symmetric. The axial-velocity component also shows how the velocity varies per length of the filter chamber while the normal velocity component shows flow injection into the chamber is a function y.

Using (3.208) in (3.81) and thereafter differentiating with respect to x, we arrive at the following result

$$P_{xy} = G_r\theta_x \cos(\gamma). \tag{3.210}$$

Substituting (3.208) into (3.80) and differentiating with respect to y, we obtain

$$\begin{aligned} &\frac{d^4G}{dy^4}x + \alpha\left[y\frac{d^3G}{dy^3} + 2\frac{d^2G}{dy^2}\right]x + R_eG\frac{d^3G}{dy^3}x - \frac{R_e}{K}\frac{d^2G}{dy^2}x - Re\frac{d^2G}{dy^2}Nx \\ &-R_e\frac{dG}{dy}\frac{d^2G}{dy^2}x - R_eP_{xy} = 0. \end{aligned} \tag{3.211}$$

Using equation (3.210) in (3.211), yields

$$\frac{d^4G}{dy^4}x + \alpha\left[y\frac{d^3G}{dy^3} + 2\frac{d^2G}{dy^2}\right]x + R_eG\frac{d^3G}{dy^3}x - \frac{R_e}{K}\frac{d^2G}{dy^2}x - Re\frac{d^2G}{dy^2}Nx$$
$$-R_e\frac{dG}{dy}\frac{d^2G}{dy^2}x - R_eG_r\theta_x\cos(\gamma) = 0, \tag{3.212}$$

which after differentiating with respect to x twice, becomes

$$R_eG_r\theta_{xxx}\cos(\gamma) = 0. \tag{3.213}$$

Since the fluid is injected into the filter chamber (forced convection), density varies due to temperature difference (natural convection) which generates fluid motion and the filter chamber is inclined, thus R_e, G_r and $\cos(\gamma)$ cannot be zero from equation (3.213), therefore

$$\theta_{xxx} = 0. \tag{3.214}$$

Integrating equation (3.214) with respect to x twice, we get

$$\theta_x = A(y)x + B(y), \tag{3.215}$$

where $A(y)$ and $B(y)$ are arbitrary functions of y. Substituting equation (3.215) into equation (3.212) and comparing powers of x from the resultant equation, we get the following equations:

$$x^0 \; : \; R_eG_rB(y)\cos(\gamma) = 0, \tag{3.216}$$
$$x^1 \; : \; \frac{d^4G}{dy^4} + \alpha\left[y\frac{d^3G}{dy^3} + 2\frac{d^2G}{dy^2}\right] + R_eG\frac{d^3G}{dy^3} - \frac{R_e}{K}\frac{d^2G}{dy^2} - Re\frac{d^2G}{dy^2}N$$
$$-R_e\frac{dG}{dy}\frac{d^2G}{dy^2} - R_eG_rA(y)\cos(\gamma) = 0. \tag{3.217}$$

From equation (3.216) it can be noticed that

$$B(y) = 0.$$

Since other parameters are non-zero constants. Thus, the ordinary differential equation for momentum becomes

$$\frac{d^4G}{dy^4} + \alpha\left[y\frac{d^3G}{dy^3} + 2\frac{d^2G}{dy^2}\right] + R_eG\frac{d^3G}{dy^3} - \frac{R_e}{K}\frac{d^2G}{dy^2} - Re\frac{d^2G}{dy^2}N$$
$$-R_e\frac{dG}{dy}\frac{d^2G}{dy^2} - R_eG_rA(y)\cos(\gamma) = 0. \tag{3.218}$$

Using expression for $\theta = \tau(x, y)$ from (3.197) and (3.208) into (3.82), we get the steady state regimes of temperature as follows

$$x\frac{dG}{dy}\frac{\partial \tau}{\partial x} - G\frac{\partial \tau}{\partial y} - \frac{1}{P_r R_e}\left(\frac{\partial^2 \tau}{\partial x^2} + \frac{\partial^2 \tau}{\partial y^2}\right) - \frac{4R}{P_r R_e}\frac{\partial^2 \tau}{\partial y^2} - J\left(x\frac{dG}{dy}\right)^2 = 0. \tag{3.219}$$

Also equation (3.215), becomes

$$\theta_x = A(y)x \tag{3.220}$$

since $B(y) = 0$. Integrating equation (3.220) with respect to x, we get

$$\theta = \frac{x^2}{2}A(y) + C(y). \tag{3.221}$$

Using the boundary condition (iii) at $x = 0$, we get $C(y) = 0$. Since the temperature is zero due to insulated wall at $x = 0$, the temperature (3.221) becomes

$$\theta = \frac{x^2}{2}A(y) \tag{3.222}$$

which confirms the parabolic nature of the temperature.

Equation (3.220) can be rewritten as

$$\frac{\theta_x}{x} = A(y), \tag{3.223}$$

which shows that the temperature change per length throughout the wall of the chamber is constant with respect x and changes with y only. The above equation (3.223) illustrates the that temperature from the walls affect the system in the y-direction only. Thus, there is no diffusion of particles in the x direction ($\theta_{xx} = 0$).

Using the fact that $\theta = \tau(x, y)$ from (3.197) and (3.223), equation (3.219) takes the form

$$\frac{dG}{dy}A - G\frac{dA}{dy} - \frac{1}{P_r R_e}(1 - 4R)\frac{d^2 A}{dy^2} - 2J\left(\frac{dG}{dy}\right)^2 = 0. \tag{3.224}$$

Finally the system of ordinary differential equations representing the case study under investigation is given by

$$\begin{aligned}\frac{d^4 G}{dy^4} + \alpha\left[y\frac{d^3 G}{dy^3} + 2\frac{d^2 G}{dy^2}\right] + R_e G\frac{d^3 G}{dy^3} - \frac{R_e}{K}\frac{d^2 G}{dy^2} - Re\frac{d^2 G}{dy^2}N& \\ -R_e\frac{dG}{dy}\frac{d^2 G}{dy^2} - R_e G_r A(y)\cos(\gamma) = 0,&\end{aligned} \tag{3.225}$$

$$\frac{dG}{dy}A - G\frac{dA}{dy} - \frac{1}{P_r R_e}(1 - 4R)\frac{d^2 A}{dy^2} - 2J\left(\frac{dG}{dy}\right)^2 = 0 \tag{3.226}$$

and the boundary conditions are

$$\text{(i)}\ \frac{dG(1)}{dy}=0, \qquad \text{(ii)}\ G(1)=1, \qquad \text{(iii)}\ \frac{d^2G(0)}{dy^2}=0,$$
$$\text{(iv)}\ G(0)=0 \qquad \text{(v)}\ A(1)=1, \qquad \text{(vi)}\ \frac{dA(0)}{dy}=0. \tag{3.227}$$

3.4.2 Approximate analytical solutions

The aim of this subsection is to find the approximate-analytical solutions of equations (3.225)-(3.226) and subject to boundary conditions (3.227) using double perturbation method [7] for both momentum and energy equations. The design of the filter is such that the permeation of fluid into the filter chamber is weak. Thus, for such weak permeation (small) R_e, we assume that the approximate solutions of the velocity $G(y)$ and temperature $A(y)$ can be expanded in the series form as

$$G(y)=G_1+R_eG_2+O(R_e^2),$$
$$A(y)=A_1+R_eA_2+O(R_e^2), \tag{3.228}$$

where $G_i(y)$ and $A_i(y)$ for $i=1,2$ are independent of the parameter R_e.
Substituting (3.228) into (3.225)-(3.226) and boundary conditions (3.227), for small R_e, we get the leading order equation from momentum of the system as

$$G_1{}^{(4)}(y)+\alpha\big(yG_1{}^{(3)}(y)+2G_1''(y)\big)=0, \tag{3.229}$$

and from energy equation as

$$-\frac{A_1''(y)}{P_r}(1-4R)=0, \tag{3.230}$$

with the following boundary conditions for both velocity and energy

$$\text{(i)}\ G_1'(1)=0, \quad \text{(ii)}\ G_1(1)=1, \quad \text{(iii)}\ G_1''(0)=0, \quad \text{(iv)}\ G_1(0)=0,$$
$$\text{(v)}\ A_1(1)=1, \quad \text{(vi)}\ A_1'(0)=0. \tag{3.231}$$

First order equations are given by

$$-\cos(\gamma)G_rA_1(y)-\frac{G_1''(y)}{K}-NG_1''(y)-G_1'(y)G_1''(y)+2\alpha G_2''(y)$$
$$+G_1(y)G_1^{(3)}(y)+y\alpha G_2^{(3)}(y)+G_2^{(4)}(y)=0, \tag{3.232}$$

$$-G_1(y)A_1'(y) + 2A_1(y)G_1'(y) + \frac{4R}{P_r}A_2''(y) - \frac{A_2''(y)}{P_r} - 2J(G_1'(y))^2 = 0, \tag{3.233}$$

with the following boundary conditions

$$\begin{gathered}\text{(i) } G_2'(1) = 0, \qquad \text{(ii) } G_2(1) = 0, \qquad \text{(iii) } G_2''(0) = 0, \quad \text{(iv) } G_2(0) = 0, \\ \text{(v) } A_2(1) = 0, \quad \text{(vi) } A_2'(0) = 0.\end{gathered} \tag{3.234}$$

Since the walls dilate slowly at a constant rate and energy generated by natural convection is small. Thus for small α and G_r, the parameters α and G_r are used as secondary perturbation parameters for velocity $G_1(y)$ and temperature $A_1(y)$ respectively. Similarly $G_1(y)$ and $A_1(y)$ takes the forms

$$G_1(y) = G_{10}(y) + \alpha G_{11}(y) + O(\alpha^2) \tag{3.235}$$

and

$$A_1(y) = A_{10}(y) + G_r A_{11}(y) + O(G_r^2). \tag{3.236}$$

Substituting equations arising from secondary perturbation parameters (3.235) and (3.236) into the leading order equations of R_e (3.229) and (3.230) respectively, yields the leading order equations in wall dilation rate (α) and Grashof number (G_r) as

$$G_{10}^{(4)}(y) = 0, \tag{3.237}$$

$$-\frac{A_{10}''(y)}{P_r} + \frac{4RA_{10}''(y)}{P_r} = 0. \tag{3.238}$$

Similarly the appropriate boundary conditions becomes

$$\begin{gathered}\text{(i) } G_{10}'(1) = 0, \qquad \text{(ii) } G_{10}(1) = 0, \qquad \text{(iii) } G_{10}''(0) = 0, \\ \text{(iv) } G_{10}(0) = 0, \qquad \text{(v) } A_{10}(1) = 1, \qquad \text{(vi) } A_{10}'(0) = 0.\end{gathered} \tag{3.239}$$

The first order equations arising from secondary perturbation parameters, wall dilation rate (α) and Grashof (G_r) yield

$$2G_{10}''(y) + yG_{10}^{(3)}(y) + G_{11}^{(4)}(y) = 0, \tag{3.240}$$

$$-\frac{A_{11}''(y)}{P_r} + \frac{4RA_{11}''(y)}{P_r} = 0, \tag{3.241}$$

with boundary conditions

$$\text{(i) } G_{11}'(1) = 0, \qquad \text{(ii) } G_{11}(1) = 0, \qquad \text{(iii) } G_{11}''(0) = 0,$$
$$\text{(iv) } G_{11}(0) = 0, \qquad \text{(v) } A_{11}(1) = 0, \qquad \text{(vi) } A_{11}'(0) = 0. \tag{3.242}$$

Solving equation (3.237) subject to the boundary conditions (3.239), gives

$$G_{10}(y) = \frac{1}{2}\left(3y - y^3\right). \tag{3.243}$$

Similarly solving equation (3.238) along with boundary conditions (3.239), we obtain

$$A_{10}(y) = 1. \tag{3.244}$$

The solutions of equations (3.240)-(3.241) and subject to boundary conditions (3.242) with the aid of (3.243) and (3.244) is given by

$$G_{11}(y) = \frac{3}{40}\left(y - 2y^3 + y^5\right) \tag{3.245}$$

and

$$A_{11}(y) = 0 \tag{3.246}$$

respectively. Substituting (3.243) and (3.245) into (3.235), gives the leading order term of velocity as

$$G_1(y) = \frac{1}{2}(3y - y^3) + \frac{3}{40}\alpha\left(y - 2y^3 + y^5\right). \tag{3.247}$$

Similarly from (3.244) and (3.246), equation (3.236) yields the leading order term of temperature

$$A_1(y) = 1. \tag{3.248}$$

To evaluate the first order solution of the velocity $G_2(y)$, the secondary perturbation parameter α yields velocity $G_2(y)$ as

$$G_2(y) = G_{20}(y) + \alpha G_{21}(y) + O(\alpha^2). \tag{3.249}$$

Using (3.247) and (3.249) into the first order equation (3.232) together with the boundary conditions (3.234), the leading order equation in wall dilation rate (α) yields

$$G_{20}^4(y) - \cos(\gamma)G_r A_{10}(y) + \frac{3y}{K} + 3Ny - 3y^3 = 0 \tag{3.250}$$

with the following boundary conditions

$$\text{(i) } G'_{20}(1)=0, \quad \text{(ii) } G_{20}(1)=0, \quad \text{(iii) } G''_{20}(0)=0, \quad \text{(iv) } G_{20}(0)=0. \tag{3.251}$$

Substituting (3.244) into (3.250), we get

$$G^4_{20}(y) - \cos(\gamma)G_r + \frac{3y}{K} + 3Ny - 3y^3 \tag{3.252}$$

which gives the following solution

$$\begin{aligned} G_{20}(y) &= \frac{1}{1680K}\Big(-42y + 2532Ky - 42KNy + 84y^3 - 858Ky^3 + 84KNy^3 \\ &\quad -42y^5 - 42KNy^5 + 6Ky^7 + \big(35Ky - 105Ky^3 + 70Ky^4\big)\cos(\gamma)G_r\Big) \end{aligned} \tag{3.253}$$

that satisfies boundary conditions (3.251). Similarly the first order equation in wall dilation rate (α), yields

$$\begin{aligned} G^{(4)}_{21}(y) + yG^{(3)}_{20}(y) + 2G''_{20}(y) + \frac{9y}{10K} + \frac{9Ny}{10} + \frac{27y^3}{10} - \frac{3y^3}{2K} \\ -\frac{3Ny^3}{2} + \frac{9y^5}{10} = 0 \end{aligned} \tag{3.254}$$

and the boundary conditions

$$\text{(i) } G'_{21}(1)=0, \quad \text{(ii) } G_{21}(1)=0, \quad \text{(iii) } G''_{21}(0)=0, \quad \text{(iv) } G_{21}(0)=0. \tag{3.255}$$

Using equations (3.248), (3.253) and the boundary condition (3.255), gives the solution of (3.254) as

$$\begin{aligned} G_{21}(y) &= \frac{1}{100800K}\Big(6879Ky - 552y - 552KNy + 1584y^3 - 14212Ky^3 \\ &\quad +1584KNy^3 - 1512y^5 + 7722Ky^5 - 1512KNy^5 - 324Ky^7 + 480KNy^7 \\ &\quad -65Ky^9 + \big(2205y - 6790y^3 + 4200y^4 + 945y^5 - 560y^6\big)K\cos\gamma G_r\Big). \end{aligned} \tag{3.256}$$

Substituting (3.253) and (3.256) into (3.249), yields the first order velocity term as

$$\begin{aligned} G_2(y) &= \frac{1}{1680K}\Big(-42y + 2532Ky - 42KNy + 84y^3 - 858Ky^3 + 84KNy^3 \\ &\quad -42y^5 - 42KNy^5 + 6Ky^7 + \big(35y - 105y^3 + 70y^4\big)K\cos(\gamma)G_r\Big) \\ &\quad +\frac{\alpha}{100800K}\Big(6879Ky - 552y - 552KNy + 1584y^3 - 14212Ky^3 \\ &\quad +1584KNy^3 - 1512y^5 + 7722Ky^5 - 1512KNy^5 - 324Ky^7 + 480KNy^7 \\ &\quad -65Ky^9 + \big(2205y - 6790y^3 + 4200y^4 + 945y^5 - 560y^6\big)K\cos\gamma G_r\Big). \end{aligned}$$

Finally the fluid velocity inside the filter chamber is given by

$$\begin{aligned} G(y) &= \frac{1}{2}\left(3y - y^3\right) + \frac{3}{40}\left(y - 2y^3 + y^5\right)\alpha + \frac{1}{1680K}\Bigg(- 42y + 2532Ky \\ & -42KNy + 84y^3 - 858Ky^3 + 84KNy^3 - 42y^5 - 42KNy^5 + 6Ky^7 \\ & +35Ky\cos(\gamma)G_r - 105Ky^3\cos(\gamma)G_r + 70Ky^4\cos(\gamma)G_r\Bigg) \\ & +\frac{\alpha}{100800K}\Bigg(6879Ky - 552y - 552KNy + 1584y^3 - 14212Ky^3 + 1584KNy^3 \\ & -1512y^5 + 7722Ky^5 - 1512KNy^5 + 480y^7 - 324Ky^7 + 480KNy^7 \\ & -65Ky^9 + \left(2205y - 6790y^3 + 4200y^4 + 945y^5 - 560y^6\right)K\cos(\gamma)G_r\Bigg)R_e. \end{aligned} \tag{3.257}$$

The leading quantity of temperature $A_2(y)$ takes the form

$$A_2(y) = A_{20}(y) + G_rA_{21}(y) + O(G_r^2). \tag{3.258}$$

Substituting (3.258) into (3.233), yields the leading equation of Grashof number (G_r) as

$$2G'_{10}(y) - \frac{A''_{20}(y)}{P_r} + \frac{4RA''_{20}(y)}{P_r} - 2J\big(G'_{10}(y)\big)^2 = 0 \tag{3.259}$$

and boundary conditions

$$\text{(i) } A'_{20}(0) = 0, \qquad \text{(ii) } A_{20}(1) = 0. \tag{3.260}$$

The first order equation gives

$$2G'_{11}(y) - \frac{A''_{21}(y)}{P_r} + \frac{4RA''_{21}(y)}{P_r} - 4JG''_{10}(y)G''_{11}(y) = 0 \tag{3.261}$$

with boundary conditions

$$\text{(i) } A'_{21}(0) = 0, \qquad \text{(ii) } A_{21}(1) = 0. \tag{3.262}$$

Using equation (3.243) into (3.259) and thereafter integrating the resulting equation together with conditions (3.260), gives

$$A_{20}(y) = \frac{P_r}{20(4R-1)}\left(25 - 33J - 30y^2 + 45Jy^2 - 5y^4 - 15Jy^4 + 3Jy^6\right). \tag{3.263}$$

Similarly equations (3.245), (3.261), (3.263) and boundary conditions (3.262), yields

$$\begin{aligned} A_{21}(y) &= -\frac{P_r}{5600(4R-1)}\Bigg(140 - 489J - 420y^2 + 1260Jy^2 + 420y^4 \\ & -1470Jy^4 - 140y^6 + 924Jy^6 - 225Jy^8\Bigg). \end{aligned} \tag{3.264}$$

Thus, substituting equations (3.263) and (3.264) into (3.258), gives the first order of temperature as

$$\begin{aligned}A_2(y) &= \frac{P_r}{20(4R-1)}\left(25-33J-30y^2+45Jy^2-5y^4-15Jy^4+3Jy^6\right)\\&-\frac{G_rP_r}{5600(4R-1)}\Big(140-489J-420y^2+1260Jy^2+420y^4 \qquad (3.265)\\&-1470Jy^4-140y^6+924Jy^6-225Jy^8\Big). \qquad (3.266)\end{aligned}$$

Finally the temperature distribution inside the filter chamber is given by

$$\begin{aligned}A(y) &= 1+R_e\Big[\frac{P_r}{20(4R-1)}\left(25-33J-30y^2+45Jy^2-5y^4-15Jy^4+3Jy^6\right)\\&-\frac{G_rP_r}{5600(4R-1)}\Big(140-489J-420y^2+1260Jy^2+420y^4 \qquad (3.267)\\&-1470Jy^4-140y^6+924Jy^6-225Jy^8\Big)\Big]. \qquad (3.268)\end{aligned}$$

Pressure Drop

Using the dimensionless stream function (3.208) into equation (3.81), gives the normal pressure as

$$P_y=\frac{1}{K}G(y)+G_r\theta\cos(\gamma)-G(y)G'(y)-\frac{1}{R_e}\left[\alpha yG'(y)+G''(y)\right]. \qquad (3.269)$$

Similarly, the axial pressure is obtained by substituting the dimensionless stream function (3.208) into equation (3.80), thus

$$\begin{aligned}P_x &= x\Big[G(y)G''(y)+\frac{1}{R_e}\left(\alpha G'(y)+\alpha yG''(y)+G'''(y)\right)\\&-\frac{1}{K}G'(y)-NG'(y)-(G'(y))^2\Big]. \qquad (3.270)\end{aligned}$$

From the design of the filter chamber, the left side is closed with an insulated wall which create the force per area of the wall (P_a) and the right side of the chamber is opened to atmospheric pressure ($P_{at}\approx 0$), then the pressure drop along the x-axis can be written as

$$\Delta P_x = P_a - P_{at}. \qquad (3.271)$$

Therefore from equation (3.270) the resulting axial pressure becomes

$$\begin{aligned} P_a &= \frac{x^2}{2}\Big[G(y)G''(y) + \frac{1}{R_e}\big(\alpha G'(y) + \alpha y G''(y) + G'''(y)\big) \\ &\quad -\frac{1}{K}G'(y) - NG'(y) - (G'(y))^2\Big]. \end{aligned} \tag{3.272}$$

This confirms that axial pressure drop behaviour, at any value for y, takes a parabolic profile [2].

3.5 Results and Discussions

In this section analysis of graphical representations of flow dynamics and heat distributions that lead to optimal permeates production during filtration process are presented. In order to obtain the optimal out flow (optimal permeates) effects of various parameters arising from the flow dynamics, heat transfer and filter chamber design such as wall dilation rate (α), Prandtl number (P_r), Grashof number (G_r), permeation Reynolds number (R_e), Stuart number (N), radiation parameter (R), Joule parameter (J) and porosity parameter (K) are investigated. A detailed interpretation of the axial-velocity, temperature distribution, axial and normal pressure distributions are used to understand the physics (dynamics) of the problem which are important during the design phase of filters. The results obtained are verified by comparing them with other works reported in the literature.

3.5.1 Axial flow velocity under the influence of various parameters

In this subsection analysis is carried out to understand the influence of various parameters affecting momentum equation (3.225) during filtration process, by analysing graphical representations of the velocity of the system given by equation (3.257).

Effects of wall dilation rate α on the fluid inside the filter chamber

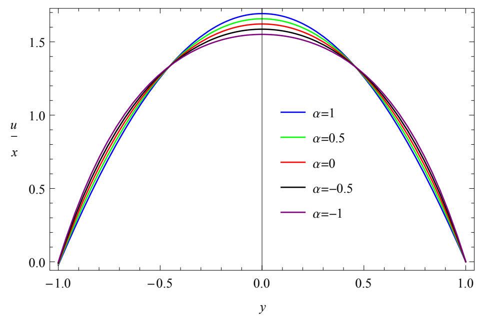

Figure 3.3: Axial-velocity profiles over a range of α at fixed values of $K = 0.1$, $N = 10$, $G_r = 2$, $R_e = 0.12$ and $\gamma = 30$.

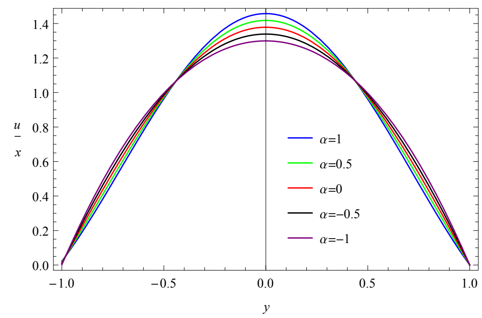

Figure 3.4: Axial-velocity profiles over a range of α at fixed values of $K = 0.1$, $N = 10$, $G_r = 2$, $R_e = -0.12$ and $\gamma = 30$.

Figures 3.3 and **3.4** show that for expansion ($\alpha > 0$), the axial-velocity increases towards the centre and decreases towards the chamber walls when filter chamber volume increases due to expansion for both fluid injection and suction. Also for contraction ($\alpha < 0$), figures illustrate that the axial-velocity decreases towards the centre and increases towards the chamber walls when chamber volume decreases due to contraction for both fluid injection and suction. The results are in good agreement with the results in [20]. It can be seen that the velocity of the fluid is higher when fluid is injected inside the filter chamber (**figure 3.3**) compared to sucking fluid out of the chamber (**figure 3.4**). Thus, more space (expansion) and fluid injection is needed to produce more permeates. The above figures show that sucking fluid from the chamber is not ideal during filtration process since it decreases the outflow.

Effects of Reynolds number R_e inside the filter chamber

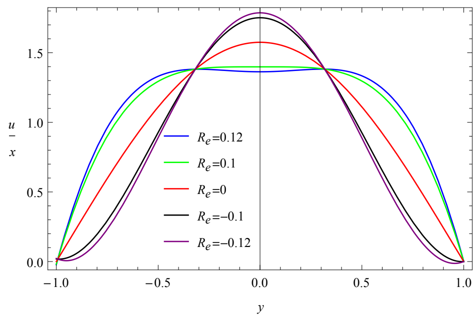

Figure 3.5: Axial-velocity profiles over a range of R_e at fixed values of $\alpha = 1$, $K = 0.01$, $N = 10$, $G_r = 2$, and $\gamma = 30$.

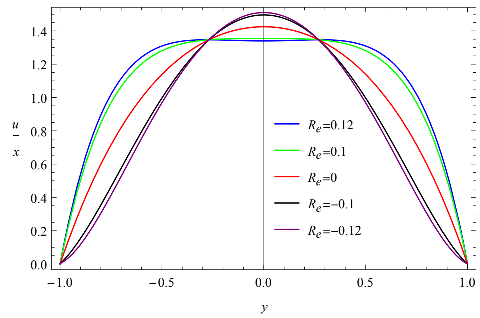

Figure 3.6: Axial-velocity profiles over a range of R_e at fixed values of $\alpha = -1$, $K = 0.01$, $N = 10$, $G_r = 2$, and $\gamma = 30$.

Figures 3.5 and **3.6** show that for fluid injection ($R_e > 0$), the axial-velocity increases towards the chamber walls and decreases towards the centre for both contracting and expanding filter chamber. Also for fluid suction ($R_e < 0$), the axial-velocity increases towards the centre and decreases towards the filter chamber walls for both contracting and expanding filter chamber. The analysis agrees with results found in [38]. It can be seen that the fluid moves at high speed/velocity when chamber walls expand (**figure 3.5**) compared to when chamber walls contract (**figure 3.6**). To produce more permeates, more filter chamber space (expansion) is ideal and fluid injection. Both figures show that injection yields more permeates at a low speed whereas suction yields less permeates faster compared to injection.

Effects of Porosity parameter K of the medium inside the filter chamber

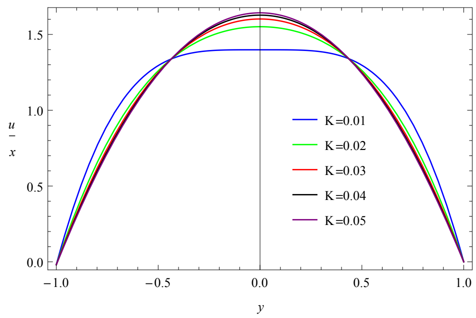

Figure 3.7: Axial-velocity profiles over a range of K at fixed values of $\alpha = 1$, $N = 10$, $G_r = 2$, $R_e = 0.1$, and $\gamma = 30$.

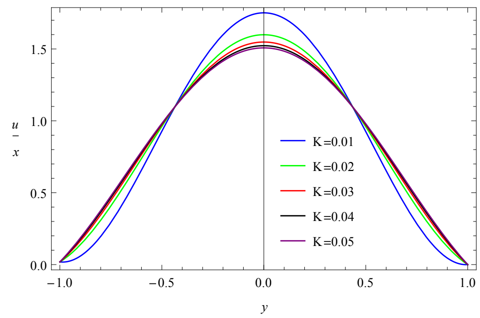

Figure 3.8: Axial-velocity profiles over a range of K at fixed values of $\alpha = 1$, $N = 10$, $G_r = 2$, $R_e = -0.1$, and $\gamma = 30$.

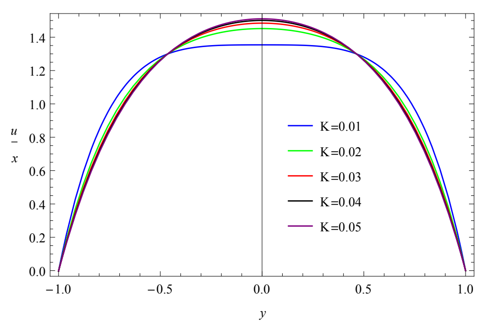

Figure 3.9: Axial-velocity profiles over a range of K at fixed values of $\alpha = -1$, $N = 10$, $G_r = 2$, $R_e = 0.1$, and $\gamma = 30$.

Figures 3.7 and **3.8** show that for poroisty (K), the increases in pore size leads to the increase in axial-velocity towards the centre of the chamber and the decrease in axial-velocity towards the filter chamber walls for fluid injection (**figures 3.7**). The increases in pore size leads to the decrease in axial-velocity towards the centre of the chamber and the increase towards the filter chamber walls for fluid suction (**figure 3.8**). For both contraction (**figures 3.7**) and expansion (**figures 3.9**), the increases in pore size leads to the increase in axial-velocity increases towards the centre and the decrease towards the filter chamber walls for fluid injection. This behaviour is due to the fact that the increase in porosity along with fluid injection allows more fluid flow inside the chamber which leads to the increase in axial-velocity while the increase in porosity for fluid suction means that fluid can be easily sucked out of the filter chamber, thus fluid velocity decreases towards the centre with the increase in pores size. For the system to produce more permeates while filtering particles effectively, it is ideal to inject fluid, maximize the chamber volume (expansion) and the pore sizes must be small during filtration process.

Effects of inclination angle γ of the filter chamber

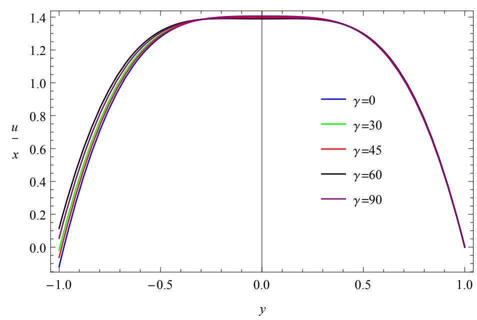

Figure 3.10: Axial-velocity profiles over a range of γ at fixed values of $\alpha = 1$, $K = 0.01$, $N = 10$, $G_r = 2$ and $R_e = 0.1$.

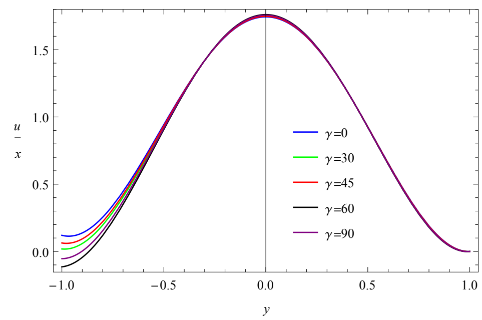

Figure 3.11: Axial-velocity profiles over a range of γ at fixed values of $\alpha = 1$, $K = 0.01$, $N = 10$, $G_r = 2$ and $R_e = -0.1$.

Figure 3.10 shows that the system produces more permeates at a slow rate when fluid is injected inside the chamber with no inclination. Both figures show that inclining the chamber more while injecting fluid into the system leads to the increase velocity since buoyancy effects decrease with the increase in inclination. This also indicates that the system produces less permeates fast when fluid is sucked out of the chamber with no inclination. Thus fluid injection is needed to produce more permeates. Both figures show that angle of inclination affects the flow velocity towards the bottom of the chamber only. The figure also indicate that the increase in angle of inclination of the filter chamber decreases the axial-velocity towards the center and increases the axial-velocity near the bottom when fluid is injected inside the filter chamber. To produce more permeates, fluid injection in the filter chamber positioned perpendicular ($\gamma = 90^o$ vertical) is ideal for this design. Illustrates that the increase in angle of inclination of the filter chamber increases the axial-velocity towards the center of the filter chamber and decreases velocity near the chamber walls creating the reverse flow during fluid suction. The system will produce less permeates fast when fluid is sucked and filter chamber angle increases to ($\gamma = 90^o$ vertical).

Effects of Stuart number N inside the filter chamber

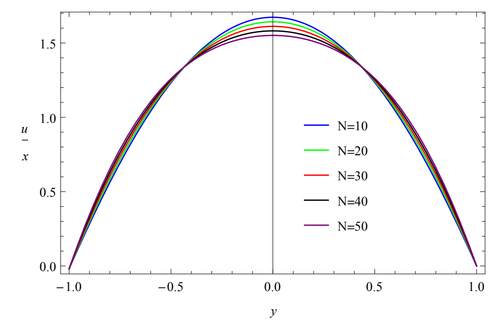

Figure 3.12: Axial-velocity profiles over a range of of N at fixed values of $\alpha = 1$, $K = 0.1$, $G_r = 2$, $R_e = 0.1$ and $\gamma = 30$.

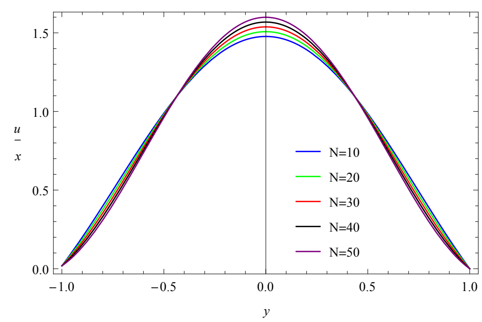

Figure 3.13: Axial-velocity profiles over a range of of N at fixed values of $\alpha = 1$, $K = 0.1$, $G_r = 2$, $R_e = -0.1$ and $\gamma = 30$.

Figures 3.12 and **3.13** show that for Stuart number (N), the increase in magnetic strength leads to the decrease in axial-velocity towards the centre and the increase towards the walls of the filter chamber when injecting fluid (**figures 3.12**). Whereas during fluid suction, the increase in magnetic strength leads to the increases in axial-velocity towards the centre of the filter chamber and the decrease towards the chamber walls (**figure 3.13**). The increase in magnetic strength leads to the increase in Lorentz force which oppose fluid motion since this force develops more during fluid injection compared to suction, the system will produce more permeates slow during injection while produce less permeates fast during suction. For the system to produce more permeates, while restricting contaminated particle from entering the filter chamber fluid injection is needed together with integration of magnetic field during filtration process.

Effects of Grashof number G_r inside the filter chamber

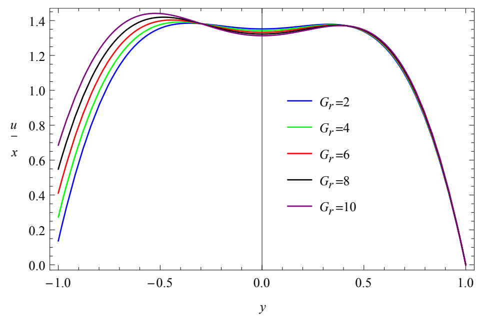

Figure 3.14: Axial-velocity profiles over a range of G_r at fixed values of $\alpha = 1$, $K = 0.1$, $N = 50$, $R_e = 0.12$ and $\gamma = 60$.

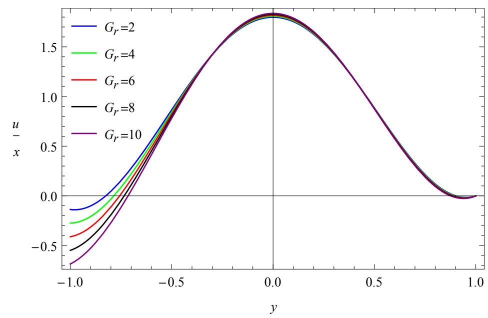

Figure 3.15: Axial-velocity profiles over a range of G_r at fixed values of $\alpha = 1$, $K = 0.1$, $N = 50$, $R_e = -0.12$ and $\gamma = 60$.

Figures 3.14 and **3.15** show that for Grashof number (Gr), the increase in Grashof number due density variation arising from temperature difference leads high axial-velocity towards the chamber walls and low velocity towards the centre of the chamber for injection (**figures 3.14**). The increase in Grashof number leads to the increase in axial-velocity towards the centre and the decrease towards the chamber walls for suction (**figure 3.15**). The increase in Grashof number leads to movement of more dense fluid particles to the bottom of the filter chamber and the less dense particle to move towards the top of the filter chamber for both injection and suction. Thus the effects of Grashof number will affect the flow at bottom since gravity pulls the more dense particle towards the bottom.

3.5.2 Temperature distribution under the effects of various parameters

In this subsection analysis is carried out to understand the influence of various parameters affecting the energy (3.226) during filtration process, thus studying the temperature distributions inside the filter chamber by analysing solution of energy (3.226) given by equation (3.267).

Effects of Reynolds number R_e inside the filter chamber

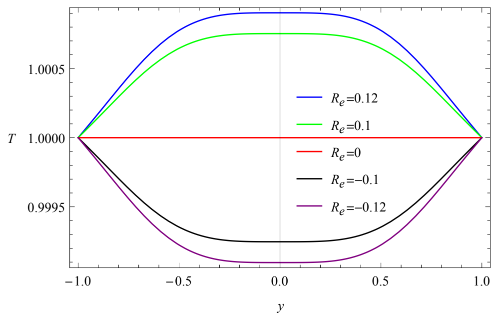

Figure 3.16: Temperature distributions over a range of R_e at fixed values of $\alpha = 1$, $G_r = 10$, $J = 0.5$, $P_r = 0.6$ and $R = 5$.

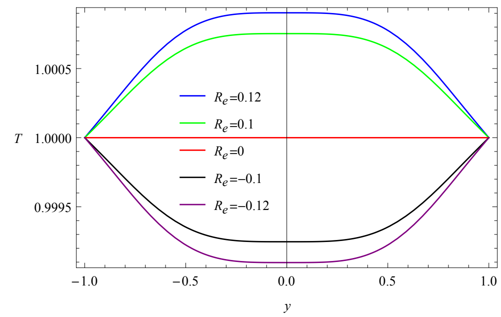

Figure 3.17: Temperature distributions over a range of R_e at fixed values of $\alpha = -1$ $G_r = 10$, $J = 0.5$, $P_r = 0.6$ and $R = 5$.

Figures 3.16 and **3.17** show temperature distributions for both fluid injection and suction during expansion and contraction respectively. It can be observed that injecting fluid inside the filter chamber for both contracting or expanding the chamber, increases the temperature from the chamber walls towards the centre of the filter chamber. When fluid is sucked out of the filter chamber both figures show that the temperature decreases from the walls towards the centre of filter chamber. The increase in temperature when fluid is injected into the chamber is due work done by additional particles which increase Joule heating effect, thus increase temperature. The decrease in temperature when fluid is sucked out of the chamber is due to fact that particles decreases inside the chamber which lead to the decrease in work done by particles and decrease in Joule heating effect, thus decrease temperature. When there is no fluid injection or suction, the system does not inject or suck particles into or out of the filter chamber, this leads to same work done by the particles inside the chamber, hence there is no effects of Joule heating inside the filter chamber.

Effects of Joule heating parameter J inside the filter chamber

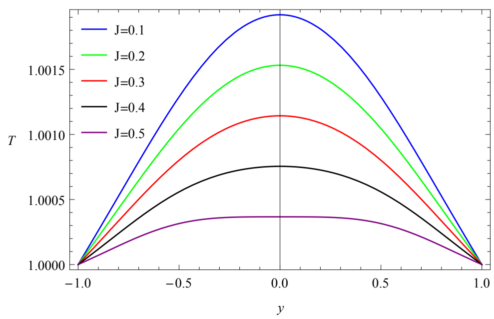

Figure 3.18: Temperature distributions over a range of J at fixed values of $\alpha = 1$, $G_r = 2$, $R = 10$, $P_r = 0.6$ and $R_e = 0.12$.

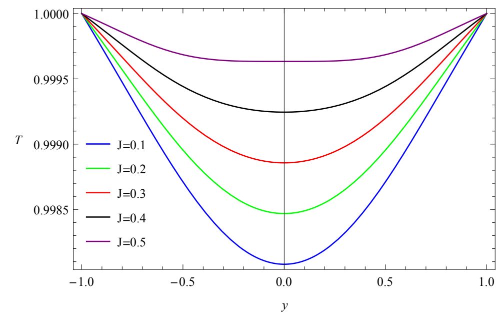

Figure 3.19: Temperature distributions over a range of J at fixed values of $\alpha = -1$, $G_r = 2$, $R = 10$, $P_r = 0.6$ and $R_e = -0.12$.

Figure 3.18 shows that when the Joule heating parameter (source) increases the fluid temperature inside the chamber decreases towards the centre of the chamber when fluid is injected inside the filter chamber. Increasing the Joule heating parameter reduces movement of particles inside the chamber which result in less energy generation by particles hence the temperature decreases. It can also be noted that for high Joule heating parameter, the temperature approximate the temperature of the chamber walls. In case of fluid suction while contracting the chamber, the temperature decreases as the Joule heating parameter increases, since sucking fluid reduce fluid particles which contribute to the net energy from the chamber, thus lead to the decrease in temperature as shown in (**figure 3.19**).

Effects of Grashof number G_r inside the filter chamber

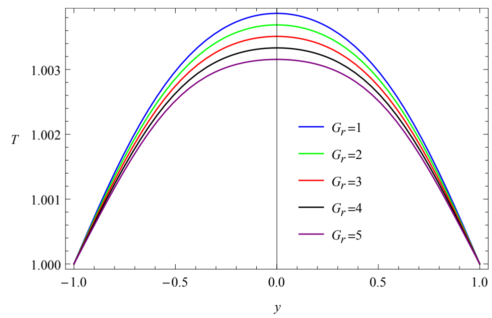

Figure 3.20: Temperaure distributions over a range of G_r at fixed value of $R_e = 0.1$, $\alpha = 1$, $P_r = 0.6$, $R = 10$ and $J = 0.5$.

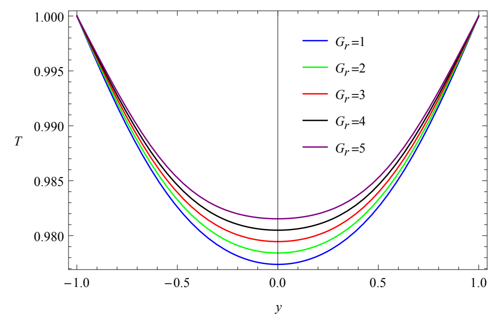

Figure 3.21: Temperaure distributions over a range of G_r at fixed value of $R_e = -0.1$, $\alpha = 1$, $P_r = 0.6$, $R = 10$ and $J = 0.5$.

Figures 3.20 and **3.21** show respectively that the increase in Grashof number increases the temperature from the chamber walls towards the centre when fluid is injected inside the filter chamber and decrease in temperature from the walls towards the centre of the filter chamber when fluid is sucked out of the filter chamber. Also (**figure 3.20**) illustrates that the temperature increase more at a lower Grashof number. The decrease in temperature when Grashof number increases is caused by the fact that for high Grashof number the fluid absorb temperature from the walls at a high rate, thus decrease fluid density. The less dense particles moves more freely inside the filter chamber with minimal internal frictional between particles as a result contribute minimal temperature. This illustrates that the temperature decreases more at a lower Grashof number. The decrease in temperature at a lower Grashof number is caused by the fact that the less dense particles (more temperature) due to high temperature decreases internal temperature during suction since temperature in taken out of the filter chamber inform of less dense particles.

Effects of Radiation R inside the filter chamber

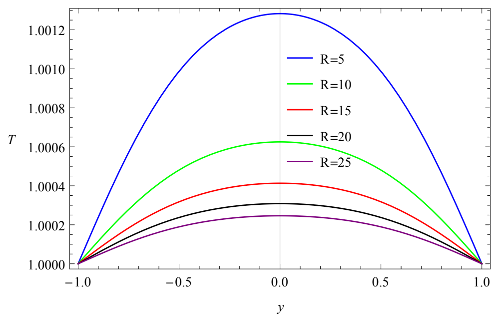

Figure 3.22: Temperature distributions over a range of R at fixed values of $\alpha = 1,\ G_r = 1,\ J = 0.5,\ P_r = 0.6$ and $R_e = 0.10$.

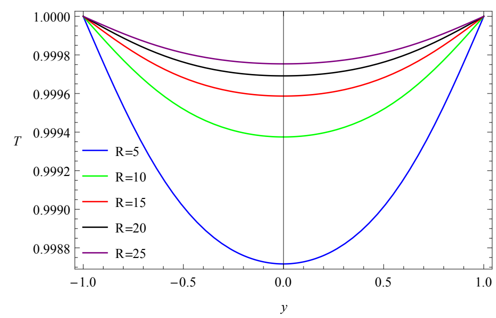

Figure 3.23: Temperature distributions over a range of R at fixed values of $\alpha = 1,\ G_r = 1,\ J = 0.5,\ P_r = 0.6$ and $R_e = -0.10$.

Figures 3.22 and **3.23** show that the increase in radiation leads to the increase in temperature from the chamber walls towards the centre when fluid is injected inside the filter chamber and the decrease in temperature from the chamber walls towards the centre of the filter chamber when fluid is sucked out of the filter chamber. Also (**figure 3.22**) illustrates that the temperature decreases more when radiation increases for fluid injection. This decrease is caused by the fact that radiating MHD fluid gives away energy in form of radiation as a results fluid temperature will decrease with increase in radiation. For fluid injection, more particles are injected and give away more energy and conserve less, thus temperature increment will be less for high radiation. **Figure 3.23** illustrates that the temperature decreases more when fluid radiates at a lower rate. Sucking out fluid leads to the decrease in temperature since heat transfer from the walls decreases when warm particles closed to chamber walls are sucked out. Also when particles radiates at lower rate they keep more energy and give away less, sucking those particle leads to more energy out of the system, thus sucking less radiative particles leads to more decrease of temperature compared more radiative particles.

Effects of Prandtl number P_r inside the filter chamber

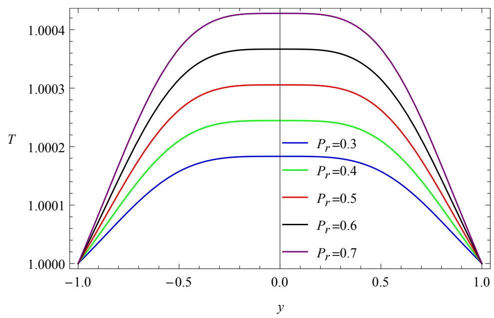

Figure 3.24: Temperature distributions over a range of P_r at fixed values of $\alpha = 1,\ G_r = 10,\ J = 0.5,\ R = 10$ and $R_e = 0.10$.

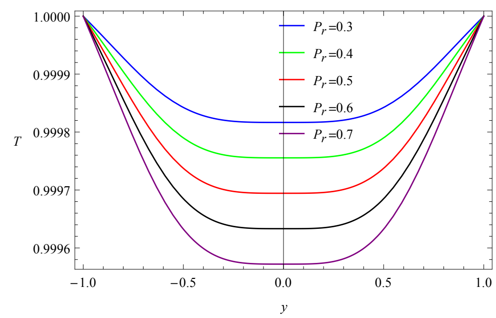

Figure 3.25: Temperature distributions over a range of P_r at fixed values of $\alpha = 1,\ G_r = 10,\ J = 0.5,\ R = 10$ and $R_e = -0.10$.

From figure **3.24** it can be observed that increasing the Prandtl number while injecting the fluid into the filter chamber leads to the increase in fluid temperature distribution towards the centre of the chamber. Due to small values of Prandtl number, the thermal diffusivity tends to dominate inside the filter chamber, which increase heat diffusion through the fluid bulk and increase temperature distribution towards the centre of the chamber. Similarly sucking fluid out of the filter chamber decrease thermal conduction of fluid particles, thus resulting in low heat diffusion hence the temperature inside the filter chamber decreases see (**figure 3.25**).

3.6 Concluding remarks

Lie symmetry analysis along with double perturbation method are used to study the flow and heat distribution inside an inclined filter channel during filtration process. The design of the filter and nature of the fluid revealed the important parameters which affect the internal flow and heat distribution during filtration process which are wall dilationn (α), Reynolds number (R_e), Grashof number (G_r), Prandtl number (P_r), Radiation number (R), angle of inclination (γ) and Joule heating parameter (J). Also proficient mathematical formation of the problem was obtained from basic conservation laws of mass, momentum and energy respectively. The findings from the study indicate that to have an optimal outflow which leads to more permeates, the following dynamics were found to be vital to maximize permeates during filtration process.

(1) **Wall dilation rate:** The increase in wall dilation rate creates more space inside the filter chamber such that the internal pressure decreases and external pressure increases in such a way that the system allows more fluid injection due to pressure difference. Thus, the work done by pressure results in more fluid inside the filter chamber which leads to more flow out (permeates) of the chamber. Since temperature is independent of wall dilation rate, the chamber walls can be moved to created optimal pressure without affecting temperature distribution of the system.

(2) **Reynolds:** To maximize production of permeates, it is ideal to inject more fluid inside the filter chamber. Suction is not ideal, since the increase in temperature decreases particles inside the filter chamber which lead to less permeates. Increasing fluid particles increases internal friction which leads to the increase in Joule heating effects and a rise in internal temperature which is ideal during filtration process since it decrease the viscous effects of the fluid as a result fluid bulk moves freely, thus optimize permeates.

(3) **Porosity:** The increase in pore size of the medium leads to more inflow into the chamber and more outflow on the other hand allows contaminations to pass through the medium which is not ideal during filtration process. To deal with this challenge while producing enough permeates, the filter design must have small medium pore size, allow only fluid injection (no suction) and have relatively big enough filter chamber space. Temperature distribution is independent of porosity effects.

(4) **Stuart:** The increase in magnetic load zone leads to a reverse flow away from the centre of the chamber while minimizing steel and ferro particles from entering the chamber or blocking the pores of the chamber walls, on the other hand it decreases the outflow. To counter the negative effects of magnetic force, more injection during operation is needed since both magnetic field and the injection act normal the surface.

(5) **Prandtl:** Momentum of the system is independent of the Prandtl number, thus Prandtl number does not affect permeates out flow. This is due to thermal boundary layer being more dominant compared to momentum boundary. For the system to maintain

good quality of the permeates, it is ideal to adjust the Prandtl number in such a way that is does not change the quality of the final product (permeates) while increasing temperature.

(6) **Grashof:** Increasing Grashof number leads to instability of fluid velocity towards the bottom of the filter chamber due to buoyancy effects. For the system to produce more permeates while injecting fluid, relative small Grashof number is needed to balance natural convection (minimize buoyancy effects).

(7) **Inclination:** To produce more permeates, the system's angle of inclination has to be 90^o (vertical) to allow gravity to act in the direction of the out flow.

(8) **Radiation:** To optimize internal temperature, lower radiation parameter is ideal during filtration process since it increases the internal fluid temperature.

(9) **Joule heating:** Similarly the increase in Joule heating parameter increases internal temperature and increases the internal work done which is ideal during filtration, thus increases permeates output.

(10) **Axial pressure:** For the system to produce more permeates the chamber walls should dilate in such a way that the work done by the movement of the chamber walls increases the axial internal pressure to produce more permeates.

Bibliography

[1] A. Ali, Y. Ali, P. Kuman, K. Babar, A. Ahmed and Z. Shah, Flow of a Nanofluid and Heat Transfer in Channel With Contracting/Expanding Walls, IEEE Access, **7** (2019), 102427-102436.

[2] Z. Boutros, B. Minas, A. Badran, S. Hassan, Lie-group method solution for two-dimensional viscous flow between slowly expanding or contracting walls with weak permeability, Applied Mathematical Modelling, **31** (2007), 1092-1108.

[3] P.K.Kameswaran, M.Narayana, P.Sibanda and P.V.S.N. Murthy, Hydromagnetic nanofluid flow due to a stretching or shrinking sheet with viscous dissipation and chemical reaction effects, Int. J. Heat and Mass Transfer, **55** (2012), 7587-7595.

[4] G. W. Bluman and S. Kumei, Symmetries and Differential Equations, Springer, New York, (1989).

[5] B. Matebese, A. Adem, M.Khalique, T. Hayat, Two-dimensional flow in a deformable channel with porous medium and variable magnetic field, Math. Comput. Appl., **31** (2010), 674-684.

[6] F. S. Ibrahim, M. A. Mansour and M. A. A. Hamad, Lie-group analysis of radiative and magnetic field effects on free convection and mass transfer flow past a semi-infinite vertical flat plate, Electronic J. Differential Equations, **39** (2005), 1-17.

[7] G. Magalakwe, and C.M Khalique, Symmetry methods of flow and heat transfer between slowly expanding or contracting walls, Mathematical problems in Engineering, Volume 2013, Article ID 137930, 10 pages.

[8] H. Stephani, Differential Equations. Thier solutions using symmetries, Cambridge University Press, Cambridge, 1989.

[9] N. H. Ibragimov, Elementary Lie Group Analysis and Ordinary Differential Equations, John Wiley and Sons, Chichester, 1999.

[10] L. V. Ovsiannikov, Group Analysis of Differential Equations, Academic Press, New York, 1982.

[11] P. J. Olver, Applications of Lie Groups to Differential Equations, Springer-Verlag, New York, 1993.

[12] N.H. Ibragimov, CRC Handbook of Lie Group Analysis of Differential Equations, Vols. 1-3, CRC Press, Boca Raton, Florida, 1994-1996.

[13] I. G. Currie, Fundamental Mechanics of fluids, 4th Edition, CRC Press, New York.

[14] J. M Burger, A mathematical model illustrating the theory of turbulence. Adv. Appl. Mech, **1** (1948), 171-199.

[15] A. S. Berman, "Laminar flow in channels with porous walls," J. Appl. Phys, **24** (1953), 1232-1235.

[16] J. R. Sellars, "Laminar flow in channels with porous walls at high suction Reynolds numbers," *J. Appl. Phys*, **26** (4) (1955), 489-490.

[17] G. Taylor, "Fluid flow in regions bounded by porous surfaces," A, Math. Phys. Sci, **234** (1199) (1956), 456-475.

[18] R. M. Terrill, "Laminar flow in a uniformly porous channel with large injection," Aeronautical Quart, **16** (4) (1965), 323-332.

[19] S. Uchida and H. Aoki, "Unsteady flows in a semi-infinite contracting or expanding pipe," J. Fluid Mech, **82** (2) (1977), 371-387.

[20] E. C. Dauenhauer and J. Majdalani, "Unsteady flows in semi-infinite expanding channels with wall injection," in Proc. AIAA, (1999), 3523-3599.

[21] E.C. Dauenhauer and J. Majdalani, Exact self similarity solution of the Navier-Stokes equations for a deformable channel with wall suction or injection, in Proc. AIAA, **3588** (2001), 1-11.

[22] J. Majdalani, C. Zhou and C.A. Dawson, Two-dimensional viscous flow between slowly expanding or contracting walls with weak permeability, J. Biomech, **35** (2002), 1399-1403.

[23] D.B. Ingham, I. Pop, Transport Phenomena in Porous Media, Elsevier, London, 2005.

[24] D.A. Nield, A. Bejan, Convection in Porous Media, Springer, Berlin, 2012.

[25] M. Mahmood, M.A. Hossain, S. Asghar and T. Hayat, Application of homotopy pertubation method to deformable channel with wall suction and injection in a porous medium, Int. J. Nonlinear Sci. Numerical Simulation, **9** (2008), 195-206.

[26] M. Sheikholeslami, S. Abelman, Two phase simulation of nanofluid flow and heat transfer in an annulus in the presence of an axial magnetic field, IEEE Transactions on Nanotechnology, **14** (3) (2015), 561-569.

[27] M. Sheikholeslami, F.B. Sheykholeslami, S. Khoshhal, H. Mola-Abasia, D.D. Ganji, H.B. Rokni, Effect of magnetic field on Cuewater nanofluid heat transfer using GMDH-type neural network, Neural Computing and Applications, **25** (2014), 171-178.

[28] M. Sheikholeslami, H.R. Ashorynejad, G. Domairry, I. Hashim, Flow and heat transfer of Cu-water nanofluid between a stretching sheet and a porous surface in a rotating system, Journal of Applied Mathematics, Volume 2012, Article ID 421320, 18 pages.

[29] M. Sheikholeslami, D.D. Ganji, M.M. Rashidi, Magnetic field effect on unsteady nanofluid flow and heat transfer using Buongiorno model, Journal of Magnetism and Magnetic Materials, **416** (2016), 164-173.

[30] M. Sheikholeslami, M. Azimi, D.D. Ganji, Application of differential transformation method for nanofluid flow in a semi-permeable channel considering magnetic field effect, International Journal for Computational Methods in Engineering Science and Mechanics, **16** (4) (2015), 246-255.

[31] M. Sheikholeslami, P. Jalili, D.D. Ganji, Magnetic field effect on nanofluid flow between two circular cylinders using AGM, Alexandria Engineering Journal, **52** (2) (2018), 587-594.

[32] M. Sheikholeslami, S.A. Shehzad, Magnetohydrodynamic nanofluid convective flow in a porous enclosure by means of LBM, International Journal of Heat and Mass Transfer, **113** (2017), 796-805.

[33] M.G.Reddy, P.Padma and B.Shankar, Effects of viscous dissipation and heat source on unsteady MHD flow over a stretching sheet, Ain Shams Engineering Journal, **6** (4) (2015), 1195-1201.

[34] M. Sajid, S.A. Iqbal, M. Naveed, Z. Abbas, Joule heating and magnetohydrodynamic effects on ferrofluid(Fe3O4) flow in a semi-porous curved channel, Journal of Molecular Liquids, **222** (2016), 1115-1120.

[35] M. Subhas Abel, K. A. Kumar and R. Ravikumara, MHD Flow and Heat Transfer with Effects of Buoyancy, Viscous and Joules Dissipation over a Nonlinear Vertical Stretching Porous Sheet with Partial Slip. Engineering, **3** (2011), 285-291.

[36] J. P. Grandet, T. Alboussiere and R. Moreau, "Buoyancy Driven Convection in a Rectangular Enclosure with a Transverse Magnetic Field," International Journal of Heat and Mass Transfer, **35** (4) (1992), 741-748.

[37] H. M. Duwairi and R. A. Damseh, "Magnetohydrodynamic Natural Convection Heat Transfer from Radiate Vertical Porous Surfaces", Heat and Mass Transfer, **40** (10) (2004), 787-792.

[38] M. Sheikholeslami, M. Hatami, G. Domairry, Numerical simulation of two phase unsteady nanofluid flow and heat transfer between parallel plates in presence of time dependent magnetic field, Journal of the Taiwan Institute of Chemical Engineers, **46** (2015), 43-50.

[39] M. Sheikholeslami, S. Abelman, D.D. Ganji, Numerical simulation of MHD nanofluid flow and heat transfer considering viscous dissipation, International Journal of Heat and Mass Transfer, **79** (2014), 212-222.

[40] P.R.Sharma and Sharad Sinha, Combined Effects of Viscous Dissipation and Joule Heating on Unsteady MHD Flow and Heat Transfer over a Stretching Sheet Saturated in Porous Medium, Annals of Pure and Applied Mathematics, **14** (3) (2017), 387-399.

[41] K.S. Balamurugan, J.L. Ramaprasad, Dharmaiah Gurram and V.C.C. Raju, Influence of Radiation Absorption, Viscous and Joules dissipation on MHD free Convection Chemically Reactive and Radiative Flow in a Moving Inclined Porous Plate with Temperature Dependent Heat Source, IRJES, **5** (12) (2016), 20-31.

[42] K. Vijaykumar and E. Keshava Reddy, Joule Heating and Radiation Absorption Effects on MHD convective and Chemically Reactive Flow Past and Inclined Porous Plate, IJRSI, **4** (7) (2017), 2321-2705.

[43] V. K. Kalpakides and K. G. Balassas, Symmetry groups and similarity solutions for a free convective boundary-layer problem, Int. J. Non-linear Mech, **39** (2004), 1659-1670.

[44] Abd-el-Malek MB, Badran NA , Hassan HS and Abbas HH, Lie Group Method for Studying the Heat Generation Effect on Free convection Laminar Boundary-layer Flow Over a Vertical Flat Plate, J. Gen. Lie Theory Appl., **9** (2) (2015), 9 pages.

[45] G. R. Fulford, P. Broadbridge, Idunstrial Mathematics: Case Studies in the Diffusion of Heat and Matter, Cambridge University Press, united kingdom.

[46] Y.A Cengel, A. J Ghajar, Heat and Mass transfer: Fundamenrals and Applications, 5th edition, McGraw Hill education, New York.

[47] B. Lehnert, Dynamics of charged particles, 4th Edition, Proceeding of the Third international conference on the Physics of Electronic and Atomic Collisions, London.

[48] P. H. Roberts, An introduction to magnetohydrodynamics, 4th Edition, The Whitefriars Press Ltd., Great Britain.

[49] D. J. Griffiths, Introduction to electrodynamics, 3rd Edition, Library of Congress Cataloging, United States of America.

[50] M. F. Modest, Radiative Heat Transfer, 3rd edition, Academic Press, Netherlands.

[51] F. Kreith, R. M Manglik and M. S Bohn, Principles of Heat Transfer, seventh edition, Cengage Leraning, USA.

[52] O.M. Al-Habahbeh, M. Al-Saqqa, M. Safi, T. Abo Khater, Review of magnetohydrodynamic pump applications, Alexandria Engineering Journal, **55** (2016), 1347-1358.

[53] J. Lee, P. Kandaswamy, M. Bhuvaneswari and S. Sivasankaran, Lie group analysis of radiation natural convection heat transfer past an inclined porous surface, Journal of Mechanical Science and Technology, **22** (2008), 1779-1784.